REACTIVE INTERMEDIATES IN CATALYSES BY HEME ENZYMES

Yoshio Goto

DOCTOR OF PHILOSOPHY

Department of Structural Molecular Science

School of Mathematical and Physical Science

The Graduate University for Advanced Studies

1998

CONTENTS

PART I

GENERAL INTRODUCTION

Proteins containing heme prothetic groups are present in all living organisms (Figure 1.1). They play such diverse roles as reversibly binding dioxygen for transport and storage (hemoglobin and myoglobin), transfereing electrons one at a time in membraneous respiratory chains (cytochromes), utilizing peroxides (catalases and peroxidases), and acting as terminal component in multienzyme systems involved in hydroxylations (cytochrome P450) (Table 1.1).[1]

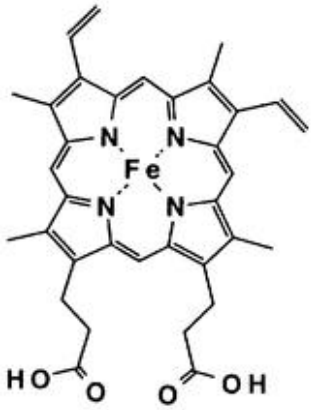

Figure 1.1 Protoheme IX

In hemoglobin and myoglobin, the dioxygen binding site undergoes structural changes upon O_2 binding. For hemoglobin, these structural changes trigger subtle movements of the protein side chains that lead to cooperativity in the uptake of dioxygen.[2] Cytochromes undergo redox transformations in the process of electron transfer without catalyzing an overall chemical change in a substrate molecule. Catalases and peroxidases catalyze the reaction generally described as follows:[1,3]

$$AH_2 + ROOH \longrightarrow ROH + H_2O + A$$

where AH_2 = phenols, aryl and alkyl amines, hydroquinones, ascorbate, or glutathione.

Table 1.1 Biological functions of hemoproteins.[4]

Biological function	Hemoprotein
O_2 transportation	Hemoglobin, myoglobin
Respiratory chain	Cytochrome oxidase
Monooxygenation	Cytochrome P450
H_2O_2 activation	Peroxidase
H_2O_2 dismutation	Catalase
NO synthesis	NO synthase
NO reduction	P450nor
Heme metabolism	Heme oxygenase

Catalases destroy H_2O_2 (i.e., $AH_2 = H_2O_2$ and $ROOH = H_2O_2$) in a bimolecular dismutation where the second molecule serves as electron donor to reduce the first molecule.

$$2\ H_2O_2 \longrightarrow O_2 + 2\ H_2O$$

In contrast, peroxidases serve in polyaromatic biosyntheses, i.e., during cooxidation of phenols and amines, phenolic and aromatic amine radicals are generated and these radicals can couple and/or polymerize to form polyphenolic products.[5] From a variety of experiments with different peroxidases and catalase, two spectroscopically discrete intermediates, called compounds I and II, have been well characterized as two and one electron oxidized forms from the resting state, respectively (Scheme 1.1).[3,6]

Cytochromes P450 are enzymes catalyzing many oxidative metabolisms of foreign compounds and biosynthesis of steroids (Table 1.2).[7] X-ray crystal structures of several cytochromes P450 are now available (see Part II, Chapter 3).[8] The active species responsible for most of these oxidation reactions catalyzed by cytochromes P450 has

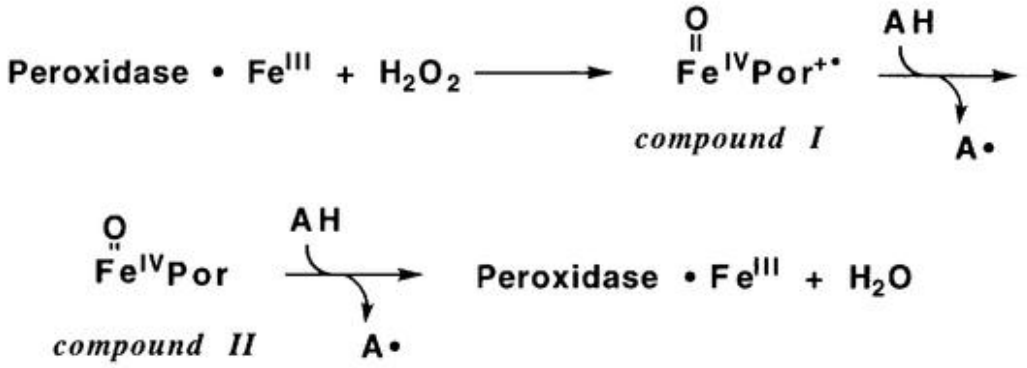

Scheme 1.1 Sequential one electron oxidation of substrates by peroxidases.

been postulated to be an oxoferryl porphyrin π-cation radical, equivalent to compound I intermediate in the peroxidase reaction cycle. Scheme 1.2 shows a proposed mechanism of oxygen activation by cytochromes P450: (1) incorporation of a substrate to the resting ferric state of the active site of the enzyme to change the spin state from low spin to high spin; (2) one electron reduction of the heme from NAD(P)H via associated reductase enzymes; (3) binding of molecular oxygen to form an oxy complex; (4) the second one electron reduction of the oxy complex to give a peroxoiron(III) complex; (5) protonation of the peroxo oxygen; (6) heterolytic cleavage of O-O bond with the formation of an

Table 1.2 Various types of cytochrome P450 catalyzed reactions.[9]

Type of oxidation	substrate	Type of oxidation	substrate
Aromatic hydroxylation	3,4-Benzopyrene	S-Oxygenation	Chloropromazine
	Acetanilide		Thioanisole
	Zoxazolamine		Thiophene
Aliphatic hydroxylation	Hexobarbital	S-Dealkylation	Methylthiopurine
	Testosterone and other steroids		Phenacyl phenylsulfide
	Octane	Dehalogenation	Methoxyflurane
	Cyclohexane		halothene
Olefin	Styrene	O-Dealkylation	*p*-Nitroanisole
Epoxidation	Cyclohexene		Acetophenetidin
Aromatization	Androstenedione	N-Dealkylation	Aminopyrine
N-Hydroxylation	N-Ethylaniline		Meperidine
	Aniline		N,N-Dimethylaniline
	2-Acetylaminofluorene		N-Methylbarbital

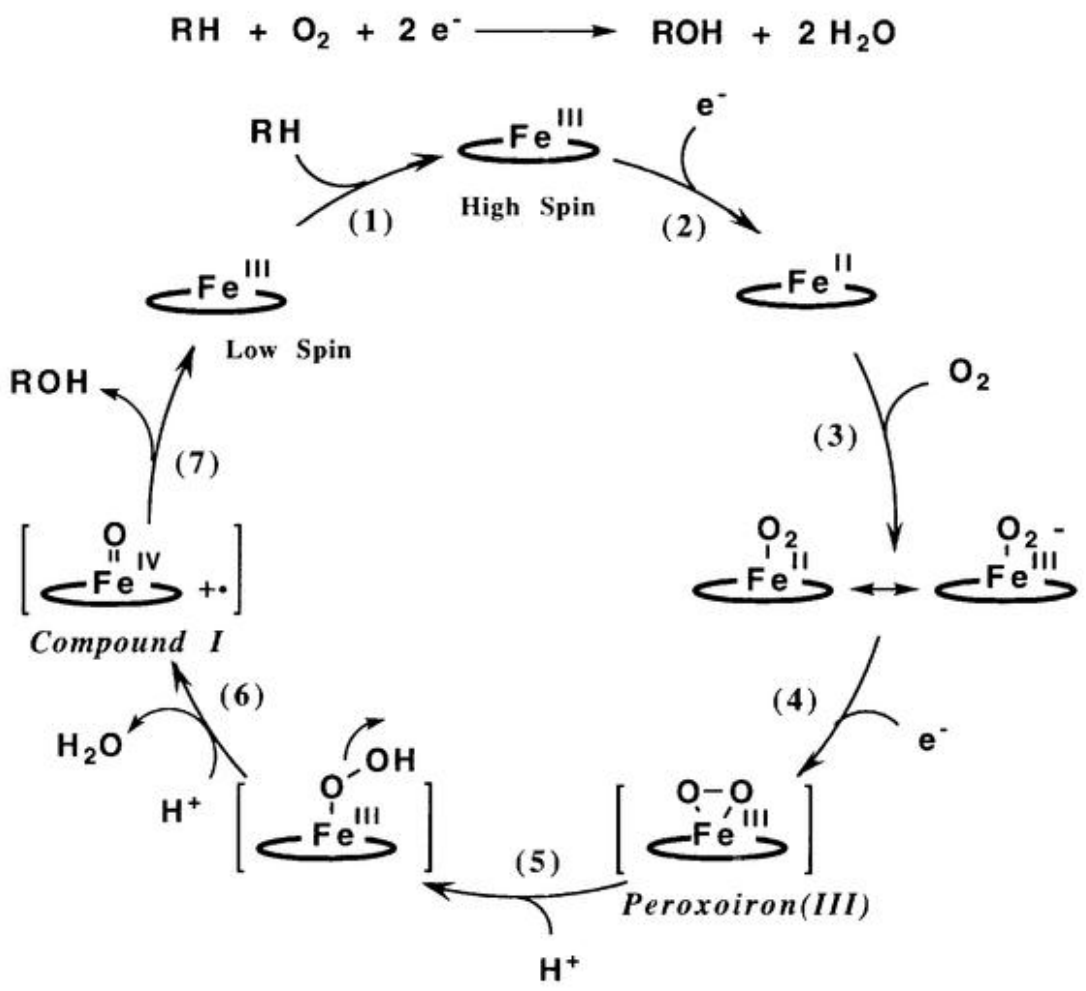

Scheme 1.2 Catalytic cycle of oxygen activation by cytochrome P450.

iron-oxo species; (7) oxygen atom transfer to the substrate; and dissociation of the product.[7,9]

The rate determining step in the oxygen activation cycle of cytochrome P450 shown in Scheme 1.2 has been known to be the reduction of the oxy form.[10] Therefore, steps (4)-(7) and intermediates shown in Scheme 1.2 are not observable, even though many attempts have been made.[11] On the other hand, synthetic porphyrin complexes have been employed to mimic the enzymatic reactions for understanding their mechanisms or for development of effective catalysts.[12] The first biomimetic oxidation system was achieved by Tabushi et al. in 1979.[13] The system consists of a Mn porphyrin complex with reducing reagent such as $NaBH_4$ to catalyze oxidation of hydrocarbons in organic

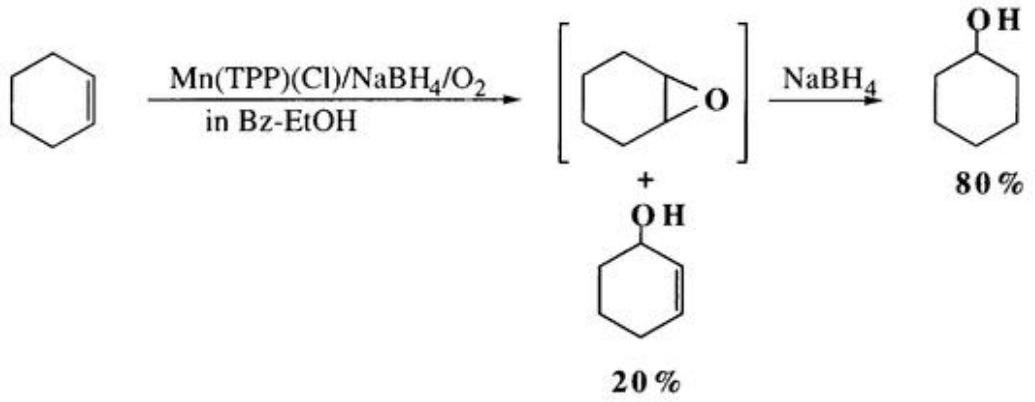

Scheme 1.3. Reductive activation of O_2 by Mn(TPP)

solvent (Scheme 1.3). Following this work, studies of many types of cytochrome P450 catalyzed reactions such as epoxidation, hydroxylation, sulfoxidation, phenol or amine oxidation have been conducted.[12, 14]

Mechanistic studies of oxygen activation by iron porphyrin complexes appear to be useful for understanding the catalytic cycle of cytochrome P450 reactions. The mechanism of compound I formation in the catalytic cycle has been examined by model systems. In 1986, Groves et al. reported the direct observation of heterolytic O-O bond cleavage of $TMPFe^{III}$(3-chloroperbenzoate) to give an oxoferryl TMP π-cation radical (Sheme 1.4).[15] The heterolytic O-O bond cleavage step was demonstrated to be an acid catalyzed reaction. In 1993, Yamaguchi et al. constructed model systems for examining push-pull effect proposed in the formation of peroxidase and P450 compound I (Figure

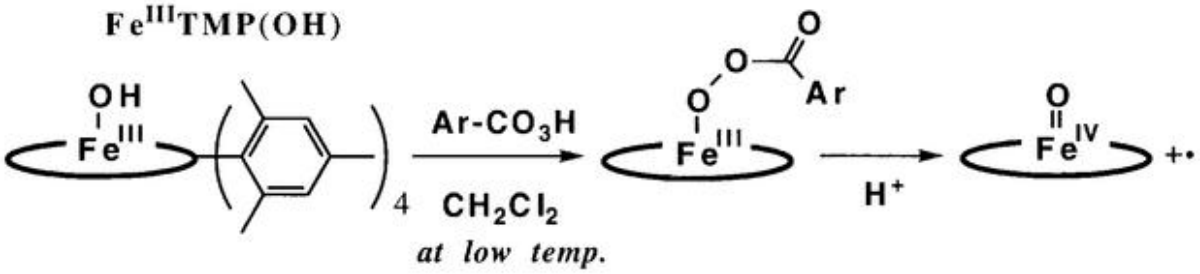

Scheme 1.4. Formation of $O=Fe^{IV}TMP^{+\bullet}$ by heterolytic O-O bond cleavage of peracid adduct.

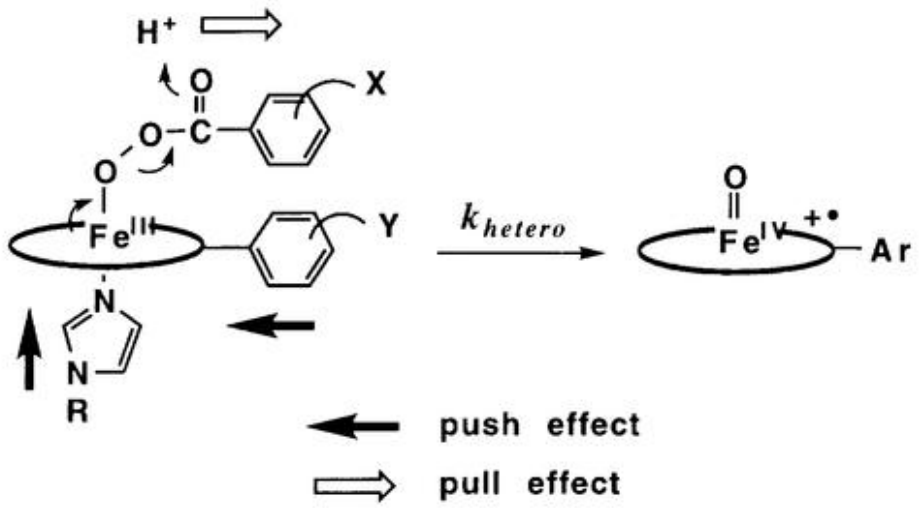

Figure 1.2 The push-pull effect for an enhancement of the heterolytic O-O bond cleavage of peracid-Fe(III) complex

1.2).[16] Watanabe et al. observed that acylperoxo-Fe(III) porphyrin complexes (**2** in Scheme 1.4) are also able to oxidize olefins to the epoxides.[17] For example, competitive epoxidation of norbornylene and α-methylstyrene with PhIO and F_5PhIO catalyzed by Fe^{III}(Por) showed oxidant dependent substrate selectivity (Table 1.3). If one assumes the $O=Fe^{IV}$ porphyrin π-cation radical to be the unique active species, oxidant dependent substrate selectivity may not be obtained. These results indicate that we must use

Table 1.3 Competitive epoxidation of norbornylene and α-methylstyrene with PhIO and F_5PhIO catalyzed by Fe^{III}Por in CH_2Cl_2 at -40°C.[17]

	Selectivity (norbornylene oxide: α-methylstyrene oxide)	
Oxidation System	Fe(TMP)	Fe(TDCPP)
F_5Ph-IO + cat. Fe^{III}(Por)(benzoate)[a]	100 : 7	100 : 28
Ph-IO + cat. Fe^{III}(Por)(benzoate)[a]	100 : 28	100 : 75
$O=Fe^{IV}$(Por)$^{+\bullet}$	100 : 8	100 : 31

[a] F_5Ph-IO (or Ph-IO) : Fe^{III}(Por)(benzoate) = 30 : 1.

Table 1.4 Enantioselective epoxidation of olefins by myoglobin mutants.

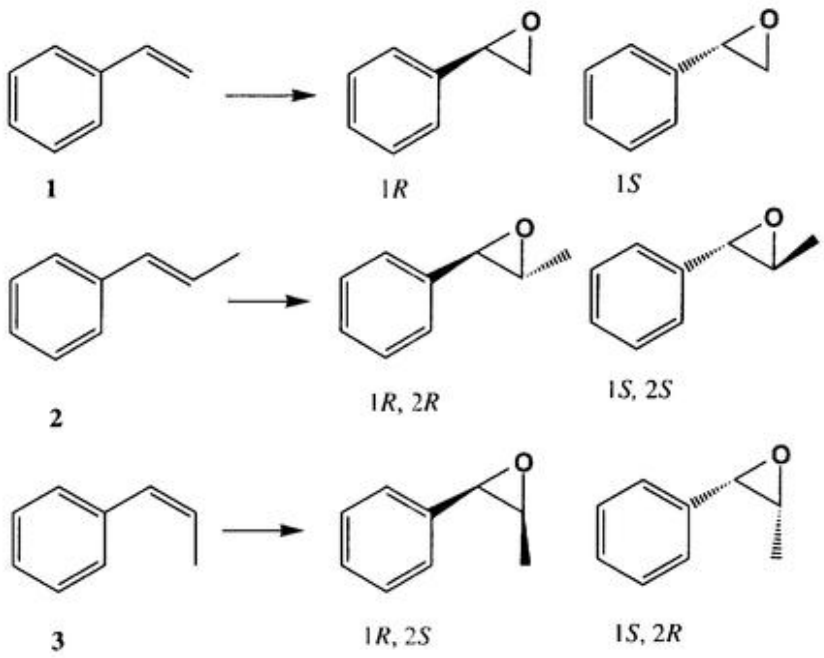

		wild type Mb		L29H/H64L Mb		F43H/H64L Mb	
		rate[a]	ee(%)	rate [a]	ee(%)	rate [a]	ee(%)
1	styrene	0.015	9 (1*R*)	0.14	80 (*R*)	4.5	68 (*R*)
2	*trans*-β-methylstyrene	0.076	39 (1*R*, 2*R*)	0.29	83 (1*R*, 2*R*)	16	96 (1*R*, 2*R*)
3	*cis*-β-methylstyrene	0.0026	3 (1*R*, 2*S*)	0.12	99 (1*R*, 2*S*)	0.15 [b]	45 (1*R*, 2*S*)

[a] The unit for rate is turnover/min.

[b] Phenylacetone was also formed in the reaction. The ratio of *cis*-epoxide : phenylacetone was 1 : 3.

well characterized reactive intermediates for the elucidation of enzymatic reactions but may not use catalytic reactions for mechanistic studies since there could be many active intermediates formed under the catalytic conditions.

On the basis of push-pull effects studied by model systems, Ozaki et al. have constructed Mb mutants in which the distal histidine has been optimally relocated to serve as general acid-base.[18] By using these mutants, myoglobin compound I was successfully prepared.[18b,c] Those compounds I have been found to carry out oxygenation of sulfides, olefins, and hydrocarbons as observed for cytochrome P450 (Table 1.4).[18a19]

Despite of these efforts, the reactivity of compound I has not been well-clarified yet. Thus, the precise reaction mechanisms of reaction of compound I with various substrates remain ambiguous. In Part II of this thesis, the reactivities of compound I in N-demethylation, sulfoxidation, and epoxidation are investigated by employing compounds I of HRP, a synthetic model complex and a myoglobin mutant. In order to make sure that the active intermediates of hemes are compound I, all the experiments have been carried out as stoichiometric reactions between substrates and compound I confirmed spectroscopically. Direct observation of the reactions between compound I and substrates by following spectral changes provides us a precise view of the reactivity of compound I. In addition, the direct observation method allows us to obtain many aspects of the reaction mechanism for the first time such as electronic effects of the substrates on the reaction rate and kinetic isotope effect on the N-demethylation.

As described above, an oxoferryl porphyrin cation radical has been believed to the reactive intermediate in most reactions catalyzed by cytochrome P450. However, some of the cytochrome P450 catalyzed reactions can not be explained if one assumes compound I to be the unique active species. Those reactions are the transformation of androgen to estrogen, lanosterol 14α-demethylation and progesterone 17α-Hydroxylation/17,20-lyation.[7] For example, P450 aromatase catalyze steroid metabolism in which androgen is converted to estrogen. Comsumption of 3 moles of O_2 and NADPH for the conversion indicates the reaction includes 3 catalytic cycles.

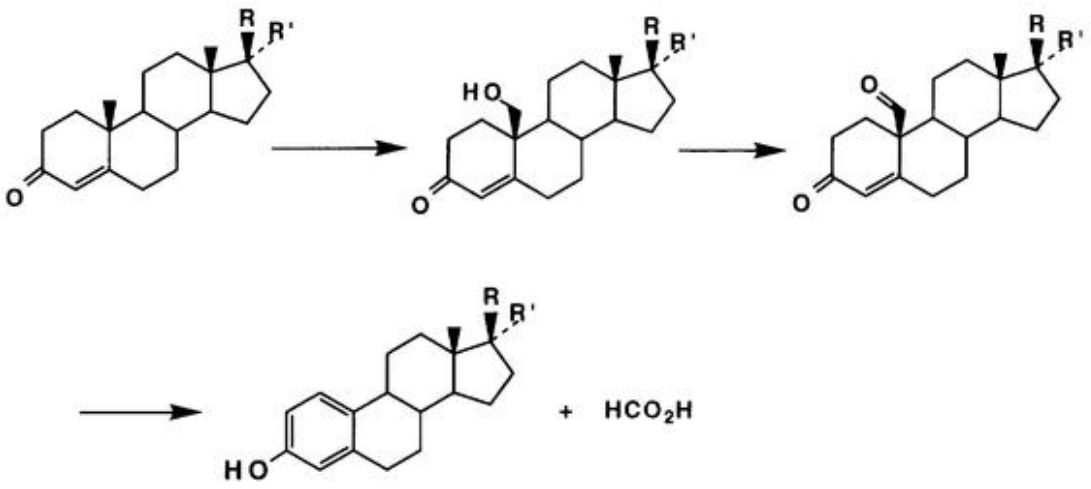

Scheme 1.5 Estrogen synthesis by cytochrome P450 aromatase.

The first and second step have been proven to be normal hydroxylation reactions of cytochrome P450. In the final step in this biological conversion, the aldehyde at the 19 position of steroid ring is eliminated to afford estrogen and a formic acid (Scheme 1.5).[7, 20] If a high-valent iron-oxo species is responsible for this reaction, aldehyde could be oxidized to give the corresponding carboxylic acid. In fact, there are reports of cytochrome P450 catalyzed aldehyde oxidations to the corresponding carboxylic acids have been reported.[7] In addition, synthetic O=Fe^{IV}porphyrin π-cation radicals have been shown to catalyze a conversion of aldehydes to carboxylic acids.[21] Thus, a peroxoiron(III) intermediate in the proposed catalytic cycle of cytochrome P450 (Scheme 1.2) has been considered as the reactive intermediate for the deformylation. However, the peroxo-Fe(III) intermediate in the catalytic cycle of cytochrome P450 is not observable as discussed above. Thus, a model system[22] is required to examine the reaciton mechanism of cytochrome P450 aromatase. Part III describes reactions of synthetic peroxoiron(III) porphyrin complexes with aldehydes.

The objective of this work is to elucidate the reaction mechanisms starting from well characterized active intermediates instead of using catalytic turnover conditions. In addition, all of the reactions examined have been monitored spectroscopically to detect possible transient intermediates by the use of low temperature stopped flow techniques.

In addition, a model complex of compound I, $O=Fe^{IV}TMP^{+\bullet}$, is observable below -50°C in CH_2Cl_2, thus, a low temperature stopped flow system was used for the thesis work (TMP = 5,19,15,20-tetramesitylporphine dianion).

REFERENCE

(1) Walsh, C. *Enzymatic Reaction Mechanisms*; W. H. Freeman and Company: San Francisco, Chapter 15, 1979.

(2) Lippard, S. J.; Berg. J. M., *Principles of Bioinorganic Chemistry*; University Science Books: California, Chapter 1, 1994.

(3) Dunford, H. B. *Peroxidases in Chemistry and Biology,* Everse, J., Everse, K.E., and Grisham, M. B. Ed., CRC Press, Boca Raton, Vol. II, Chapter 1, 1991.

(4) Ochiai, E. *Bioinorganic Chemistry: An Introduction,* Allyn and Bacon, Inc., Boston, 1977.

(5) Campa, A. *Peroxidases in Chemistry and Biology,* Everse, J., Everse, K.E., and Grisham, M. B. Ed., CRC Press, Boca Raton, Vol. II, Chapter 2, 1991.

(6) Dolphin, D.; Forman, A.; Borg, D. C.; Fajar, J.; Felton, R. H. *Proc. Natl. Acad. Sci. USA.* **1971**, *68*, 641.

(7) Ortiz de Montellano, P. R. *Cytochrome P450,* Ortiz de Montellano P. R. Ed., Plenum Press, New York, Chapter 8, Second Edition, 1995.

(8) Poulos, T. L.; Cupp-Vickery, J.; Li, H. *Cytochrome P450,* Ortiz de Montellano P.R. Ed., Plenum Press, New York, Chapter 4, Second Edition, 1995.

(9) Watanabe, Y.; Groves, J. T. *The Enzymes,* Boyer, P. D. and Sigman, D. S., Ed.; Academic Press: New York, Chapter 9, Vol. 20, 1992.

(10) a) Tyson, C.; Lipscomb, J. D.; Gunsalus, I. C. *J. Biol. Chem.* **1972**, *247*, 5777. b) Hoa, H. B.; Begard, E., Debey, P.; Gunsalus, I. C. Biochemistry, **1978**, *17*, 2835.

(11) Shimada, H.; Sligar, S. G.; Yeom, H.; Ishimura, Y. *Oxygenases and Model Systems*, Funabiki, T. Ed.,Kluwer Academic Publisher, Dordrecht, Chapter 5, 1997.

(12) Watanabe, Y. *Oxygenases and Model Systems*, Funabiki, T. Ed.,Kluwer Academic Publisher, Dordrecht, Chapter 6, 1997.

(13) Tabushi, I.; Koga, N. *J. Am. Chem. Soc.* **1979**, *101*, 6456.

(14) *Metalloporphyrins in Catalytic Oxidations,* Sheldon, R.A. Ed., Marcel Dekker, Inc., New York, 1994.

(15) Groves, J. T.; Watanabe, Y. *J. Am. Chem. Soc.* **1986**, *108*, 7834, **1988**, *110*, 8443.

(16) a) Yamaguchi, K.; Watanabe, Y.; Morishima, I. *J. Chem. Soc., Chem. Commun.* **1992**, 1709. b) Yamaguchi, K.; Watanabe, Y.; Morishima, I. *J. Am. Chem. Soc.* **1993**, *115*, 4058.

(17) Machii, K.; Watanabe, Y.; Morishima, I. *J. Am. Chem. Soc.* **1995**, *117*, 6691.

(18) a) Ozaki, S.; Matsui, T.; Watanabe, Y. *J. Am. Chem. Soc.* **1996**, *118*, 9784. b) Matsui, T.; Ozaki, S.; Watanabe, Y. *J. Biol. Chem.* **1997**, *272*, 32731. c) Ozaki, S.; Matsui, T.; Watanabe, Y. *J. Am. Chem. Soc.* **1997**, *119*, 6666.

(19) Ozaki, S.; Yang, H.-J.; Matsui, T.; Goto, Y.; Watanabe, Y. *Tetrahedron: Asymmetry,* **1999**, in press.

(20) Watanabe, Y.; Ishimura, Y. *J. Am. Chem. Soc.* **1989**, *111*, 8047.

(21) Watanabe, Y.; Takehira, K.; Shimizu, M.; Hayakawa, T.; Orita, H. *J. Chem. Soc., Chem. Commun.* **1990**, 927-928.

(22) McCandlish, E.; Miksztal, A. R.; Nappa, M.; Sprenger, A. Q.; Valentine, J. S.; Strong, J. D.; Spiro, T. G. *J. Am. Chem. Soc.* **1980**, *102*, 4268.

PART II

Reactivities of High-Valent Iron Intermediates of Heme Enzymes

CHAPTER 1

Mechanisms of N-Demethylations Catalyzed by High Valent Species of Heme Enzymes: Novel Use of Isotope Effects and Direct Observation of Intermediates

published in *J. Am. Chem. Soc.* **1998**, *120*, 10762-10763.

Yoshio Goto, Yoshihito Watanabe, Shunichi Fukuzumi, Jeffrey P. Jones and Joseph P. Dinnocenzo

ABSTRACT: Rapid kinetics have been used to determine isotope effects for the N-demethylation reactions of *p*-substituted N,N-dimethylanilines (DMAs) catalyzed by horseradish peroxidase (HRP) compound I and by O=Fe^{IV}TMP cation radical (TMP = 5,10,15,20-tetramesitylporphine dianion), a functional cytochrome P450 model. In the HRP system, stepwise reduction of compound I to the ferric state via compound II is observed. A linear correlation of the rate constants of each step with the oxidation potential of DMAs and no observation of a kinetic isotope effect on the oxidation rates is consistent with the currently accepted sequential one electron oxidation mechanism of the enzyme. The O=$Fe^{IV}$$TMP^{\bullet+}$ reaction system showed isosbestic UV-vis spectral changes to Fe^{III}TMP in the reactions with DMAs at 223K with rate constants linearly dependent on the oxidation potential of the DMAs. Thus, the demethylations catalyzed by O=$Fe^{IV}$$TMP^{\bullet+}$ also appear to proceed via electron transfer. Comparisons of observed *kinetic* and *product* deuterium isotope effect profiles have revealed that, after initial electron transfer, back electron transfer competes with hydrogen atom abstraction from the one electron-oxidized DMAs by O=Fe^{IV}TMP.

ABBREVIATIONS

compound I	an oxoferryl porphyrin π-cation radical
compound II	an oxoferryl porphyrin
DMA	N,N-dimethylaniline
equiv	equivalent
*m*CPBA	3-chloroperbenzoic acid
HRP	horseradish peroxidase
TMP	5,10,15,20-tetramesitylporphine dianion

The molecular mechanisms of amine N-demethylation by heme enzymes including peroxidases and cytochrome P450 have been studied for over three decades.[1-14] While the overall reaction mechanism consists of α–hydroxyl amine formation followed by hydrolysis to afford N-demethylated products and formaldehyde, the mechanism of α-hydroxyl amine formation is still controversial. Large intramolecular isotope effects observed for the N-demethylation of N,N-dimethylaniline (DMA)[3,5,6,13,14] have been interpreted to be due to either direct hydrogen abstraction or to proton transfer from the aminium radical, which is the one electron oxidation product of the amine. In the case of horseradish peroxidase (HRP) catalyzed oxidation of several amines, the corresponding aminium radicals have been detected by EPR to support the involvement of the electron transfer process before the α–hydroxylation (Scheme 2.1.1).[8,9] On the other hand, the mechanism of the N-demethylation catalyzed by P450 is still under debate.[3,5,13]

Scheme 2.1.1

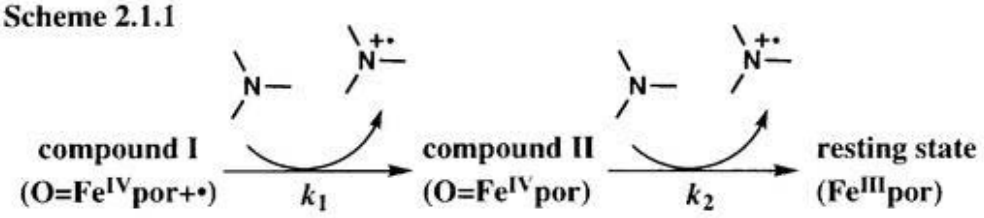

It has recently been disclosed that the magnitude of the intramolecular isotope effects on P450-catalyzed N-demethylations of substituted DMAs determined by product analysis are nearly identical to those on hydrogen atom abstraction by a *tert*-butoxyl radical (^{t}BuO•).[13,14] This result suggests the involvement of hydrogen atom abstraction in the P450 reaction. However, direct observation of the oxidation process is crucial for elucidation of the detailed mechanism. Plausible mechanisms proposed for the N-demethylation reaction are summarized in Scheme 2.1.2.

We have examined the N-demethylation mechanisms through novel isotope effect studies carried out by direct observation of the reduction of the high valent species

Scheme 2.1.2

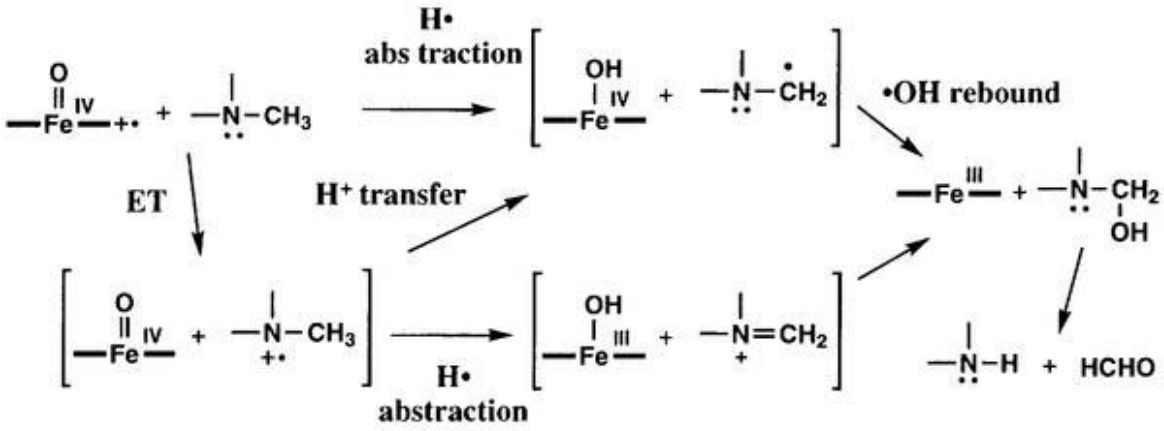

responsible for catalysis. Reactions of compound I of HRP and of O=Fe^{IV}TMP porphyrin π-cation radical, **1**, (which serves as a functional model for the active species of cytochrome P450) with a series of *p*-substituted dimethylanilines (DMAs) have been investigated. The dependence of the rate constants on the one-electron oxidation potentials of DMAs and the comparison of the *kinetic* and *product* isotope effects have allowed us to clarify the mechanism of N-demethylation.

EXPERIMENTAL PROCEDURES

Chemicals. All chemicals were purchased from Sigma-Aldrich, Wako, Nacalai Tesque and Lancaster Co., Ltd. and used without further purification unless otherwise noted. *m*CPBA was purified by washing its dichloromethane solution with phosphate buffer (pH 7.4) followed by water and then dried under reduced pressure. N,N-di(trideuteriomethyl)- and N-methyl-N-(trideuteriomethyl)-aniline derivatives were synthesized as described elsewhere.[15]

Kinetic Experiments. Kinetic experiments involving HRP compounds I and II were performed with a Hi-Tech SF-43 stopped-flow instrument. Compound I was prepared by mixing ferric HRP with a stoichiometric amount of H_2O_2. The substrate oxidation reaction was initiated by mixing with 10-100 equiv of DMA at 273 K in 50 mM phosphate buffer (pH 7.0). The reactions were performed sequentially in double-mixing mode (delay time: 10 msec, final concentration of HRP: 2.5 μM). Compound II was

prepared by addition of a stoichiometric amount of H_2O_2 to a buffer solution of ferric HRP followed by reduction with a stoichiometric amount of potassium ferricyanide. The reaction rate (k_2) of compound II and DMA was also determined from the absorbance change at 403 nm by a similar method.

Kinetic experiments on the FeTMP complex were performed with a Hi-Tech SF-43 sequential-mixing stopped-flow. In a typical run, a CH_2Cl_2 solution of $Fe^{III}TMP(OH)$ (40 μM) was mixed with an equal volume of CH_2Cl_2 containing 4 equiv of *m*CPBA and 1 equiv of 3-chlorobenzoic acid at 223K. After the confirmation of UV-vis spectrum of **1**, DMA (10-100 equiv) in CH_2Cl_2 was induced to observe spectral changes. The reaction rate constant (k_3) was determined from analysis of the change in absorbance at 413 nm.

Kinetic Isotope Effects by Product Analysis. Kinetic isotope effects by product analysis were determined by GC-MS analyses of single turnover reactions. A 1.0 mM solution of $TMPFe^{III}(OH)$ was added to a CH_2Cl_2 solution containing 1.2 equiv of *m*CPBA at 223K. After confirmation of $O=Fe^{IV}TMP^{+\bullet}$ formation, a CH_2Cl_2 solution of 10 equiv of a DMA(-CH_3,-CD_3) derivative was added. After the solution color changed to brown, trifluoroacetic anhydride was added, and the N-methylaniline derivative was detected as a trifluoroacetylamide form. The k_H/k_D value was determined with GC/SIM from the M^+ peak area ratio of trideuteriomethyl- and methyl-trifluoroacetylaniline.[15]

Redox Potentials of N,N-Dimethylanilines. Oxidation potentials of DMAs were determined by cyclic voltammetric measurements (BAS 100B/W) in CH_2Cl_2 containing 2 mM DMA derivatives and 50 mM tetrabutylammonium hexafluorophosphate at 223K with a voltage sweep rate of 100-200 mV/s.

RESULTS AND DISCUSSION

Upon mixing of HRP compound I and DMAs under stopped-flow conditions in a buffer solution (pH 7.0) at 273K, rapid formation of compound II (k_1) and the following relatively slow conversion (k_2) to the resting state were observed (Figure 2.1.1). The

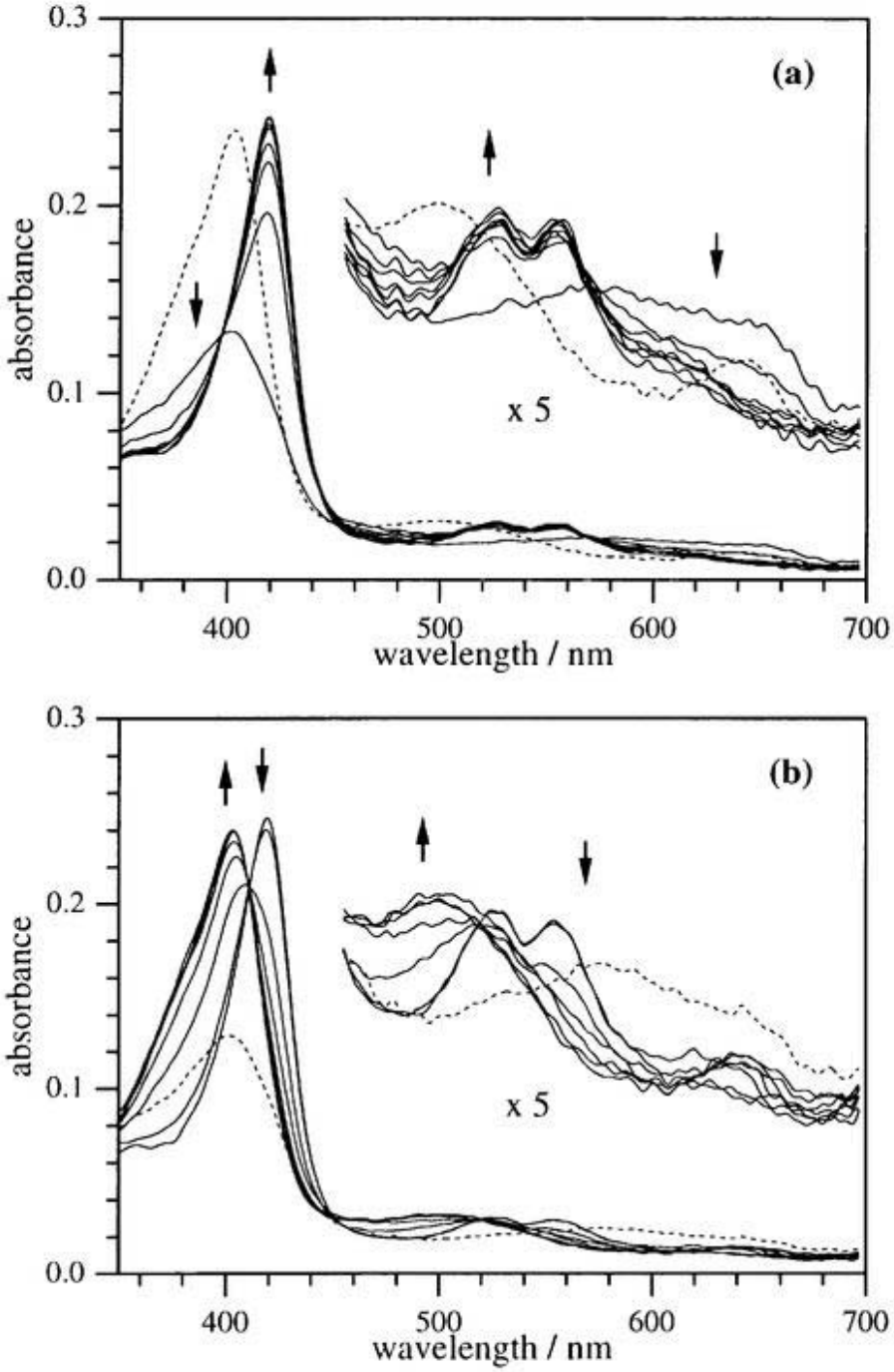

Figure 2.1.1. UV-vis spectral changes in the reaction of HRP-compound I (2.5 μM) with *p*-chloro-DMA (50 μM) in 50 mM sodium phosphate buffer at 273K: (a) the spectra were recorded at every 0.05 sec to 0.35 sec (solid line), 16.8 sec (dotted line), after mixing; (b) the spectra were recorded at (dotted line) right after mixing, (solid line) every 2.4 sec to and 19.2 sec after mixing

Table 2.1.1. Bimolecular rate constants and the isotope effects of the reactions of HRP compounds I, II and O=Fe^{IV}TMP•+ with a series of *p*-substituted DMAs.

		HRP system				TMPFe system		
p-substituent of DMA	E^0_{ox} [V vs Fc]	k_1 [b] [$M^{-1}s^{-1}$]	k_{1H}/k_{1D}	k_2 [b] [$M^{-1}s^{-1}$]	k_{2H}/k_{2D}	k_3 [b] [$M^{-1}s^{-1}$]	k_{3H}/k_{3D}	k_H/k_D
OMe	0.14	9.5 (± 0.6) x 10^7	1.0 ± 0.1	4.6 (± 0.1) x 10^6	1.0 ± 0.1	5.6 (± 0.1) x 10^7	1.3 ± 0.1	3.9 ± 0.1
Me	0.33	3.1 (± 0.1) x 10^7	1.0 ± 0.1	2.1 (± 0.1) x 10^5	1.0 ± 0.1	2.7 (± 0.1) x 10^5	1.5 ± 0.1	3.8 ± 0.1
H	0.53 [a]	6.0 (± 0.3) x 10^5	1.1 ± 0.1	1.6 (± 0.1) x 10^4	1.1 ± 0.1	1.7 (± 0.1) x 10^4	1.9 ± 0.2	2.8 ± 0.1
Cl	0.49	1.6 (± 0.1) x 10^6	1.0 ± 0.1	3.2 (± 0.2) x 10^4	1.0 ± 0.1	3.4 (± 0.1) x 10^3	1.8 ± 0.1	2.6 ± 0.1
Br	0.47	1.8 (± 0.1) x 10^6	1.0 ± 0.1	3.4 (± 0.2) x 10^4	1.0 ± 0.1	6.6 (± 0.1) x 10^3	2.0 ± 0.1	3.4 ± 0.1
CN	0.82	8.7 (± 0.8) x 10^2	1.0 ± 0.2	n.d.[c]	n.d.[c]	9.0 (± 0.4) x 10	5.5 ± 0.4	6.9 ± 0.1
NO_2	0.92	n.d.[c]	n.d.[c]	n.d.[c]	n.d.[c]	2.2 (± 0.1) x 10	5.9 ± 0.4	6.2 ± 0.9

[a] Peak potential was used because no reversible wave was detected on cyclic voltammetry. [b] determined by the experiments with DMA derivatives of which methyl groups are not deuterated. [d] not determined.

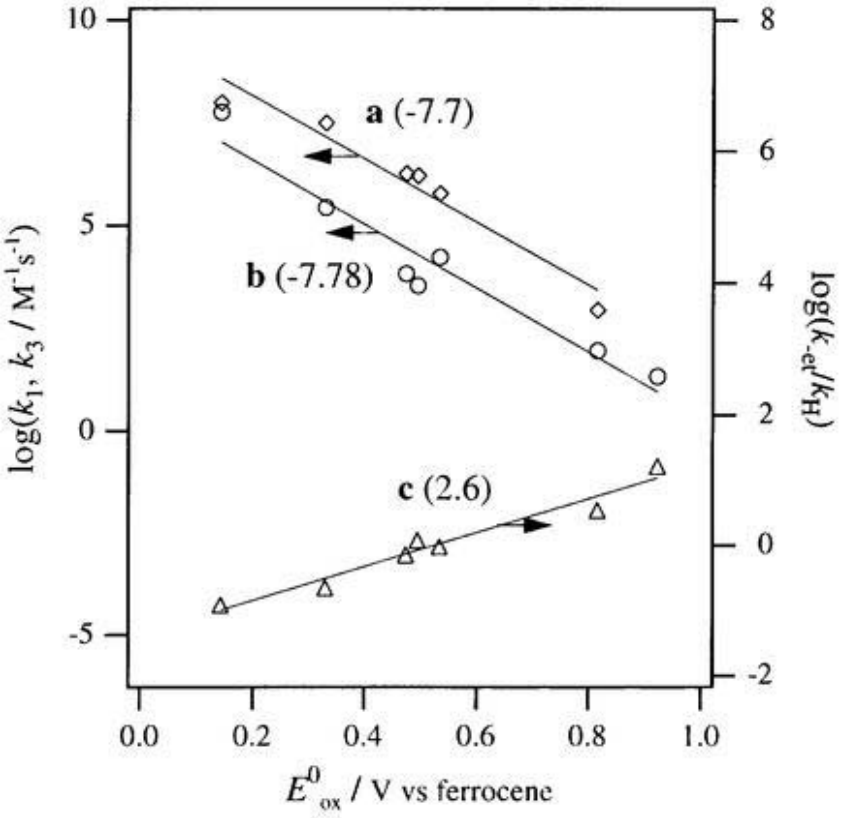

Figure 2. 1. 2. Dependence of kinetic values on the oxidation potential of DMAs (E^0_{ox}). The slopes of each line are shown in parentheses. ◇) bimolecular rate constant of HRP compound I with DMAs, k_1; ○) bimolecular rate constant of O=Fe^{IV}TMP•+ with DMAs, k_3; △) k_{-et}/k_H determined by eq 2.

same reactions were also carried out with deuterated compounds (DMAs(-CD_3)$_2$)[15] to determine k_{1D} and k_{2D}. In Table 2. 1. 1 The k_1 and k_2 values and the kinetic isotope effects (k_{1H}/k_{1D} and k_{2H}/k_{2D}) are listed together with the one-electron oxidation potentials (E^0_{ox}) of DMAs. Both the k_1 and k_2 values increase with a decrease in the E^0 value. A linear correlation between log k_1 and E^0_{ox} is shown in Figure 2.1.2(a). The linear correlation between log k_2 and E^0_{ox} was also observed. No kinetic isotope effects are observed for either k_1 or k_2. The dependence of k_1 and k_2 on E^0_{ox} and the absence of kinetic isotope effects clearly indicate that the rate-determining steps are the electron transfer from DMA to HRP compound I and compound II, respectively.

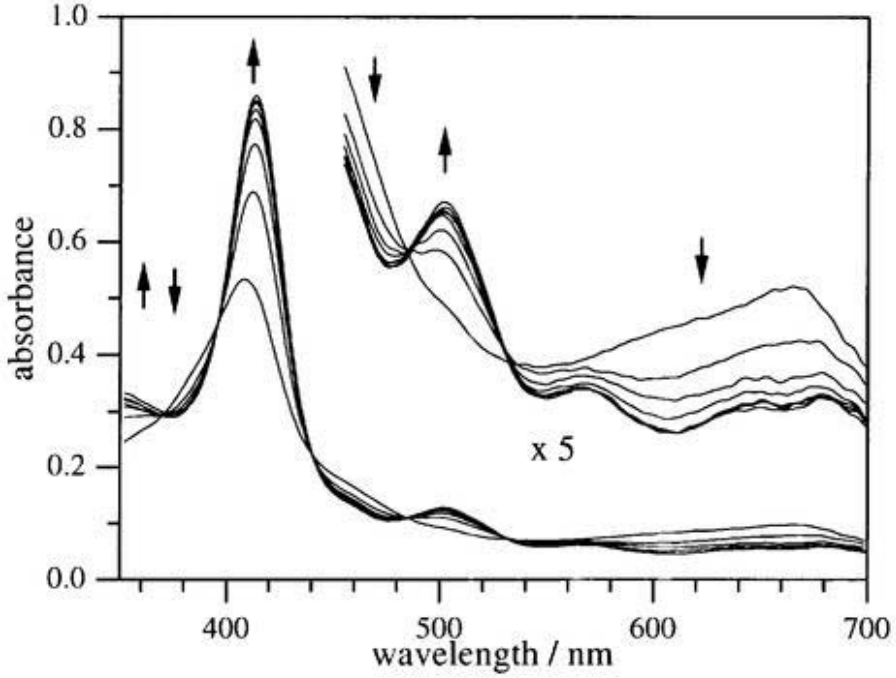

Figure 2.1.3. UV-vis spectral changes in the reaction of O=Fe^{IV}TMP$^{+\bullet}$ (5.0 μM) with DMA (100 μM) in CH_2Cl_2 at 223K. Spectra were recorded at every 24 msec to 192 msec after mixing.

While transient formation of compound I of P450 has been reported, because it is formed in a mixture of other species,[16] it has not been fully characterized. Thus, we have employed O=Fe^{IV}TMP$^{+\bullet}$ (**1**)[17] as a model complex for the proposed high valent catalytic intermediate of P450 in the kinetic measurements of N-demethylation of DMAs, since **1** is able to mimic most P450 catalyzed oxidations. The reactions of **1** with DMAs in CH_2Cl_2 at 223 K were monitored by UV-vis spectral changes of **1** and found to afford Fe^{III}TMP without observation of any intermediates (Scheme 2.1.3). The rate constants (k_3) and *kinetic isotope effects* (k_{3H}/k_{3D}) calculated on the basis of Figure 2.1.3 are summarized in Table 2.1.1. In addition, *product (intramolecular) isotope effects* (k_H/k_D) are observed in the reactions of **1** with DMAs(-CD_3, -CH_3)[15] as listed in Table 2.1.1.

Figure 2.1.2(b) shows a linear correlation between log k_3 and E^0_{ox} similar to the correlation observed for log k_1 and E^0_{ox} (Figure 2.1.2(a)). The parallel relationship between these two plots indicates that electron transfer from the DMAs is similar for HRP

and the model complex. However, the kinetic isotope effects are observed only for the reactions of O=Fe^{IV}TMP$^{\bullet+}$. The k_{3H}/k_{3D} value increases with an increase in the E^0_{ox} value to reach a value of 5.9±0.4 in the case of the *p*-nitro derivative. More importantly, there is a significant difference between the *kinetic* (k_{3H}/k_{3D}) and *product* (k_H/k_D) isotope effects (Figure 2.1.4). Coupled with the fact that no compound II is seen as an intermediate, these isotope effects suggest that there is a significant reverse electron transfer, so that any compound II-aminium radical pair formed can partition either towards products (k_H) or to initial reactants (k_{-et}) as shown in Scheme 2.1.3. The redox potential of the DMA is likely to have a significant effect on k_{-et}. Using a steady-state assumption (the compound II-radical pair is "constant" and low concentration), one can derive an expression (eq 1, *see APPENDIX*) that relates the kinetic isotope effects (k_{3H}/k_{3D}) and the product isotope effects (k_H/k_D). The product isotope effects reflect the hydrogen atom transfer step from DMA$^{\bullet+}$ to O=Fe^{IV}TMP.

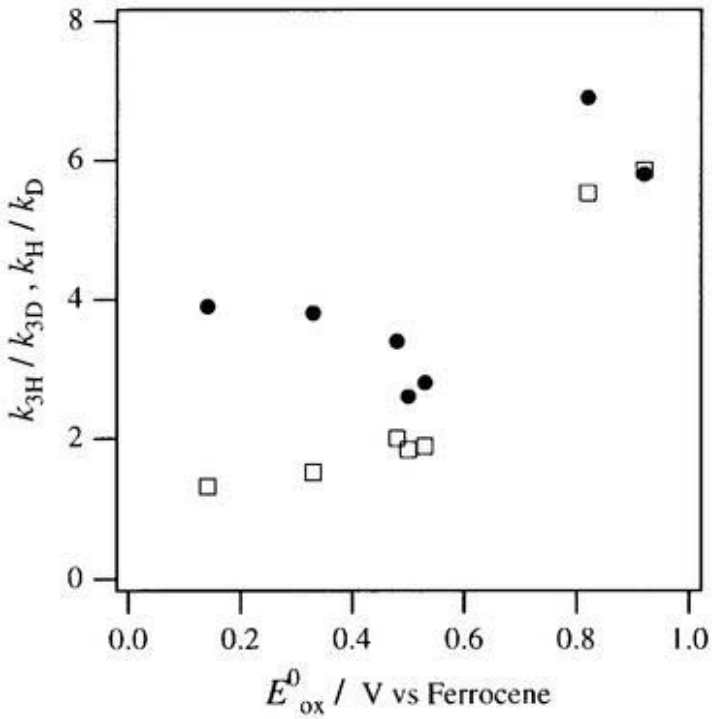

Figure 2.1.4. Dependence of the two series of kinetic isotope effects, k_{3H}/k_{3D} (□) and k_H/k_D (●) on oxidation potential of N,N-dimethylanilines.

Scheme 2.1.3

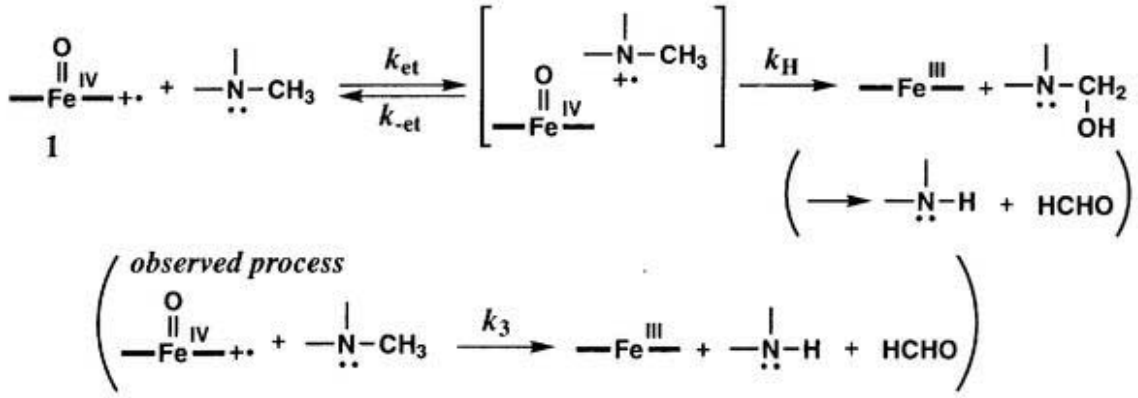

$$k_{3H}/k_{3D} = (k_H/k_D)\{(k_D/k_H) + (k_{-et}/k_H)\}/\{1 + (k_{-et}/k_H)\} \quad (1)$$

When electron transfer is the primary rate-determining step ($k_{-et}/k_H << 1$), eq 1 reduces to $k_{3H}/k_{3D} = 1$. On the other hand, when $k_{-et}/k_H >> 1$, eq 1 reduces to $k_{3H}/k_{3D} = k_H/k_D$. Thus, the difference between k_H/k_D and k_{3H}/k_{3D} should decrease with an increase in k_{-et}/k_H. The k_{-et}/k_H value can be obtained from the k_{3H}/k_{3D} and k_H/k_D values using eq 2, which is derived from eq 1. The k_{-et} value for the back electron transfer from

$$k_{-et}/k_H = \{(k_{3H}/k_{3D}) - 1\}/\{(k_H/k_D) - (k_{3H}/k_{3D})\} \quad (2)$$

$O=Fe^{IV}TMP$ to $DMA^{\bullet+}$ is expected to increase with an increase in E^0_{ox}, the one-electron reduction potential of $DMA^{\bullet+}$. On the other hand, the hydrogen atom transfer rate constant (k_H) may be less sensitive to E^0_{ox} than the back electron transfer rate constant (k_{-et}).[18] Thus, the k_{-et}/k_H value may increase with an increase in the E^0_{ox} value. In fact, such a correlation between k_{-et}/k_H and E^0_{ox} is demonstrated in Figure 2.1.2(c).

Amine oxidations by cytochrome P450 have been proposed to proceed by either an electron/proton transfer mechanism or a hydrogen atom abstraction mechanism, as shown in Scheme 2.1.2.[1,19,20] The magnitude of hydrogen/deuterium kinetic isotope effects for

amine labeled at the carbon α to nitrogen have previously used to distinguish these mechanisms.[3]

It was believed that the electron/proton transfer mechanism would show small isotope effects and that the hydrogen atom abstraction mechanism would show large isotope effects. On the basis of the fact that small isotope effects were observed for amine dealkylation by P450, an electron/proton transfer mechanism was proposed for this reaction.[3] This mechanism has been generally accepted for the past decade. Recently, measurement of isotope effects for the deprotonations of amine cation radicals and for hydrogen atom abstractions from amines showed that isotope effect magnitudes cannot distinguish the proposed P450 mechanisms.[15] Consequently, evidence for the electron/proton transfer mechanism has seriously eroded.

Dinnocenzo et al. recently proposed a potentially more discriminating approach to this mechanistic problem.[15] The strategy is to compare isotope effect profiles for model deprotonation and hydrogen abstractions to profiles from P450 oxidations to determine which model reaction best fits the P450 results. Using this approach, they found that the profiles for all the cytochrome P450 oxidations were experimentally indistinguishable from hydrogen atom abstraction profile. However, the profiles from P450 oxidations described by Dinnocenzo et al. are also similar to those of product isotope effects observed in our experiments (Table 2.1.1, Figure 2.1.4). Apparently, deuterium isotope effects obtained on the basis of intramolecular labeling experiments do not provide conclusive evidence.

In conclusion, our results are in agreement with the currently accepted mechanism in which the N-demethylation of DMAs by HRP compounds I and II both proceed via a rate-determining electron transfer step. Our results suggest that demethylation by $O{=}Fe^{IV}TMP^{\bullet+}$ also proceeds via electron transfer; however, hydrogen atom transfer from $DMAs^{\bullet+}$ to $O{=}Fe^{IV}TMP$ competes with back electron transfer, and this competition is responsible for the observed deuterium isotope effects.[21] The difference between the *kinetic* and *product* isotope effects depends on the ratio of the rate constant of the back electron transfer to that of the hydrogen transfer.

REFERENCE AND NOTES

(1) Ortiz de Montellano, P. R. *Cytochrome P450. Structure, Mechanism, and Biochemistry.;* 2nd ed.; Plenum Publishing Corporation: New York, 1995.

(2) Guengerich, F. P.; Macdonald, T. L. *Acc. Chem. Res.* **1984**, *17*, 9-16.

(3) Miwa, G. T.; Walsh, J. S.; Kedderis, G. L.; Hollenberg, P. F. *J. Biol. Chem.* **1983**, *258*, 14445-14449.

(4) Miwa, G. T.; Garland, W. A.; Hodshon, B. J.; Lu, A. Y. H.; Northrop, D. B. *J. Biol. Chem.* **1980**, *255*, 6049-6054.

(5) Guengerich, F. P.; Yun, C.-H.; Macdonald, T. L. *J. Biol. Chem.* **1996**, *271*, 27321-27329.

(6) Okazaki, O.; Guengerich, F. P. *J. Biol. Chem.* **1993**, *268*, 1546-1552.

(7) Macdonald, T. L.; Gutheim, W. G.; Martin, R. B.; Guengerich, F. P. *Biochemistry* **1989**, *28*, 2071-2077.

(8) Griffin, B. W.; Ting, P. L. *Biochemistry* **1978**, *17*, 2206-2211.

(9) Van der Zee, J.; Duling, D. R.; Mason, R. P.; Eling, T. E. *J. Biol. Chem.* **1989**, *264*, 19828-19836.

(10) Kedderis, G. L.; Hollenberg, P. F. *J. Biol. Chem.* **1983**, *258*, 8129-8138.

(11) Kedderis, G. L.; Koop, D. R.; Hollenberg, P. F. *J. Biol. Chem.* **1980**, *255*, 10174-10182.

(12) Lindsey Smith, J. R.; Mortimer, D. N. *J. Chem. Soc., Perkin Trans. 2* **1986**, 1743-1749.

(13) Manchester, J. I.; Dinnocenzo, J. P.; Higgins, L.; Jones, J. P. *J. Am. Chem. Soc.* **1997**, *119*, 5069-5070.

(14) Karki, S. B.; Dinnocenzo, J. P.; Jones, J. P.; Korzekwa, K. R. *J. Am. Chem. Soc.* **1995**, *117*, 3657-3664.

(15) Dinnocenzo, J. P.; Karki, S. B.; Jones, J. P. *J. Am. Chem. Soc.* **1993**, *115*, 7111-7116.

(16) Egawa, T.; Shimada, H.; Ishimura, Y. *Biochem. Biophys. Res. Commun.* **1994**, *201*, 1464-1469.

(17) Groves, J. T.; Watanabe, Y. *J. Am. Chem. Soc.* **1988**, *110*, 8443-8452.

(18) The energetics of hydrogen transfer consist of those for transfer of a proton and for an electron. The substitution effects on the proton and electron transfer processes may be largely canceled out, since the acidity of $DMA^{\bullet}+$ increases, but the donor ability of DMA(-H)• decreases with an increase of E^0_{ox}.

(19) Porter, T. D.; Coon, M. J. *J. Biol. Chem.* **1991**, *266*, 13469.

(20) Guengerich, F. P.; Macdonald, T. L. In *Advances in Electron Transfer Chemistry*; P. S. Mariano, Ed.; JAI Press: Greenwich, CT, 1993; Vol. 3; pp 191.

(21) Baciocchi *et al.* reported the mechanism of DMA demethylation reaction by an Fe porphyrin-iodosobenzene catalytic system at room temperature by using kinetic and product isotope effects[22] and they concluded the reaction proceeds through an electron transfer/proton transfer mechanism. We believe that our low-temperature single turnover direct observation of the compound I reaction with DMA is reliable for determination of rate constants, because the formation of compound I of polyhalogenated porphyrin iron complexes by iodosobenzene has never been observed under the condition reported by Baciocchi *et al.* For example, single turnover epoxidation by well-characterized $O=Fe^{IV}TDCPP^{+\bullet}$ (TDCPP = tetrakis(2,6-dichlorophenyl)porphine dianion) and catalytic epoxidation by an Fe^{III}TDCPP/PhIO system show very different stereo reactivity.[23] Therefore, it is necessary to characterize the active species responsible for N-demethylations of DMA reported in ref.22.

(22) Baciocchi, E.; Lanzalunga, O.; Lapi, A.; Manduchi, L. *J. Am. Chem. Soc.* **1998**, *120*, 5783-5787.

(23) Machii, K.; Watanabe, Y.; Morishima, I. *J. Am. Chem. Soc.* **1995**, *117*, 6691-6697.

APPENDIX

Derivation of eq 1.

According to Scheme 2.1.2, the following differential equations (A1 to A3) are obtained.

$$d[I]/dt = -k_{et}[I][DMA] + k_{-et}[II] \quad (A1)$$

$$d[II]/dt = k_{et}[I][DMA] - k_{-et}[II] - k_H[II] \quad (A2)$$

$$d[Fe^{III}]/dt = k_H[II] \quad (A3)$$

In eqs A1 to A3, the terms are defined as shown by A4 to A6.

I: $O=Fe^{IV}$ porphyrin π cation radical (A4)

II: $O=Fe^{IV}$ porphyrin - DMA cation radical complex (A5)

Fe^{III}: Fe^{III} porphyrin *m*-chlorobenzoate (final product) (A6)

From eqs A1 and A3 is derived eq A7.

$$-d\{[I] + [II]\}/dt = k_H[II] = d[Fe^{III}]/dt \quad (A7)$$

The steady-state approximation for II ($d[II]/dt = 0$) gives eq A8.

$$[II] = k_{et}[I][DMA]/(k_{-et} + k_H) \quad (A8)$$

Substitution of eq A8 into eq A7 gives eq A9 when $d[DMA]/dt = 0$.

$$-d[I]/dt = d[Fe^{III}]/dt = k_{et}k_H[I][DMA]/\{k_{-et} + k_H + k_{et}[DMA]\} \quad (A9)$$

The observed second-order rate constant of overall reaction k_3 is then given by eq A10 under the conditions that $k_{-et} + k_H >> k_{et}[DMA]$.

$$k_3 = k_{et}k_H/\{k_{-et} + k_H\} \quad (A10)$$

The product isotope effects (eq 1) is then obtained by the ratio k_{3H}/k_{3D} from eq A10.

CHAPTER 2

Mechanisms of Sulfoxidation Catalyzed by High-Valent Intermediates of Heme Enzymes: Electron Transfer vs Oxygen Transfer Mechanism

submitted to *J. Am. Chem. Soc.*

Yoshio Goto, Toshitaka Matsui, Shin-ichi Ozaki, Yoshihito Watanabe, and Shunichi Fukuzumi

ABSTRACT: The mechanism of sulfoxidation catalyzed by high-valent intermediates of heme enzymes has been studied by direct observation of the reduction of compounds I of horseradish peroxidase (HRP) and His64Ser myoglobin (Mb) mutant as well as $O=Fe^{IV}TMP^{+\bullet}$ (**1**) (TMP = 5,10,15,20-tetramesitylporphyrine dianion) by sulfides. The reaction of thioanisole and compound I of HRP (10 μM, pH 7.0, 298 K) gives a mixture of compound II and the resting state. The yield of sulfoxide by a stoichiometric reaction of HRP compound I with thioanisole was only 25±5%. On the other hand, the same sulfoxidation by both **1** and His64Ser Mb compound I exhibited two-electron process resulting in a 1:1 stoichiometric formation of sulfoxide. When 1,5-dithiacyclooctane (DTCO) is employed as a substrate, the reaction of His64Ser Mb compound I with DTCO exhibits rapid formation of compound II which decays to the ferric state. The logarithms of rate constants (log k_{obs}) of the reactions of each of the three systems with a series of *p*-substituted thioanisoles are correlated with the one-electron oxidation potentials (E^0_{ox}) of the sulfides. Comparison of these correlations with the established correlation between log k_{obs} and E^0_{ox} for the corresponding electron transfer reactions of substituted N,N-dimethylanilines has revealed that the reactions of compound I of HRP with sulfides proceeds via electron transfer while the sulfoxidation of sulfides by **1** and compound I of His64Ser Mb occurs via direct oxygen transfer rather than electron transfer.

ABBREVIATIONS

compound I	an oxoferryl porphyrin π-cation radical
compound II	an oxoferryl porphyrin
P450	cytochrome P450
HRP	horseradish peroxidase
Mb	myoglobin
TMP	5,10,15,20-tetramesitylporphine dianion
DTCO	1,5-dithiacyclooctane

*m*CPBA	3-chloroperbenzoic acid
TA	thioanisole
DMA	N,N-dimethylaniline
CV	cyclic voltammetry
SHACV	second harmonic AC voltammetry

INTRODUCTION

Molecular mechanisms of Cytochrome P450 (P450) catalyzed monooxygenations have been a subject of intensive studies.[1] Unfortunately, an inability to observe the active intermediate of P450 due to a preceding rate-limiting step prevents us from acquiring a complete understanding of the monooxygenation mechanisms.[2] In the case of peroxidases, compound I, an oxo-ferryl porphyrin cation radical, has been well characterized as a species equivalent to the proposed active intermediate of P450.[3] However, peroxidases typically catalyze two sequential one-electron oxidations with only a few cases of 2-electron oxygen transfer into substrates currently known.[4-7] Synthetic models of compound I, thus, have been employed for mimicking P450 catalyzed reactions and mechanistic studies.[8] Direct observation of UV-vis spectral changes for the reduction of compound I of HRP (HRP-I) and O=Fe^{IV}TMP$^{+\bullet}$ (**1**)[9] (TMP = 5,10,15,20-tetramesitylporphine dianion) by *p*-substituted N,N-dimethylanilines (DMAs) combined with the kinetic and product isotope effects have revealed that N-demethylation of DMAs by both **1** and HRP-I proceeds via a rate-determining electron transfer step.[10] We were recently able to observe compound I of a series of sperm whale Mb mutants (Mb-I) which oxidize olefins and sulfides to the corresponding oxides with high enantioselectivity.[11-13] These results inspired us to employ one of these Mb mutants as a mechanistic model system for P450.

This study reports the first kinetic data obtained by *direct* observation of the reduction of **1** and His64Ser Mb-I (H64S Mb-I)[11] by sulfides, along with that of HRP-I. A comparison of the rate constants of sulfides and those of DMAs provides an excellent opportunity to evaluate the contribution of an electron transfer pathway in the sulfoxidation catalyzed by high-valent intermediates of heme enzymes and a representative model compound.

EXPERIMENTAL PROCEDURES

Chemicals. All chemicals were purchased from Sigma-Aldrich, Wako, Nacalai Tesque and Lancaster Co., Ltd. and used without further purification unless otherwise noted. *m*CPBA was purified by washing its dichloromethane solution with phosphate buffer (pH 7.4) followed by water and then dried under reduced pressure.

Myoglobin Mutant. Sperm whale myoglobin His64Ser mutant was constructed by cassette mutagenesis. The expression vector for wild type of sperm whale myoglobin is a gift from Professor Olson (Rice University).

Kinetic Measurements. Measurements of rate constants of the reaction of HRP-I with thioanisoles were performed with a Shimadzu UV-2400 spectrophotometer equipped with a temperature controller. To a 0.5 mL of HRP solution (10 μM) in a 50 mM sodium phosphate buffer (pH 7.0) was added stoichiometric amount of H_2O_2 to generate green HRP-I at 298 K, followed by the addition of thioanisoles (50-200 equiv). The UV-vis spectra were collected at 30 sec intervals Igor Pro (WaveMetrics Inc.) was used for kinetic analyses. The rate of the reaction of HRP compound I with DTCO was determined by a stopped-flow experiment with Hi-Tech SF-43 as previously reported[10] except that measurements were performed at 298 K.

Kinetic experiments of the reduction of $O=Fe^{IV}TMP^{+\bullet}$ (**1**) were performed with the Hi-Tech SF-43 sequential-mixing stopped-flow instrument. In a typical run, a CH_2Cl_2 solution of $Fe^{III}TMP(OH)$ (40 μM) was mixed with an equal volume of CH_2Cl_2 containing 4 equiv. of 3-chloroperbenzoic acid (*m*CPBA) and 1 equiv of 3-chlorobenzoic acid at 223 K. The formation of **1** was completed in 3 min and confirmed by monitoring its UV-vis spectrum. Thioanisole (10-100 equiv) in CH_2Cl_2 was then mixed with **1** (final concentration of **1**: 10 μM), to observe spectral changes of **1** to $Fe^{III}TMP$. The reaction rate constant (k_{TMP}) was determined from analysis of the change in absorbance at 413 nm.

Kinetic experiments involving H64S Mb-I were performed on the Hi-Tech SF-43 stopped-flow instrument. H64S Mb-I was prepared by mixing H64S Mb (10 μM) with a 1.5 equiv. of *m*CPBA followed by mixing with 10-100 equiv. of sulfide at 277 K in 50 mM sodium acetate buffer (pH 5.0) with double-mixing mode (delay time: 2.1 sec, final

concentration of Mb: 2.5 μM). The rates of the reaction for the oxidation of thioanisoles were determined by fitting the change in absorbance at 409 nm with a least-squares procedure; the kinetic constants for the reduction of H64S Mb-I by thioanisoles (k_{Mb}) were determined from the slope of the rate *vs* sulfide concentration plot.

The second-order rate constants k_2 and k_3 of the reaction of H64S Mb-I with DTCO were determined by fitting the change in absorbance at 420 nm and 399 nm with a method similar to that described above, respectively. Both of the pseudo-first-order rate constants in each process were linearly dependent on the concentration of the sulfide.

Single Turnover Experiments. For a single turnover experiment, to a 3 mL of HRP-I solution prepared by the addition of 1 equiv of H_2O_2 in a 50 mM sodium phosphate buffer, pH 7.0, in a UV-cuvette was added 30 μL of 100 mM thioanisole in methanol at 298 K. The UV-vis spectral change was monitored. 2 hr following the addition of the substrate, benzophenone was added as an internal standard and the products were extracted with hexane for HPLC analysis as previously reported.[6] A standard curve prepared with authentic sulfoxide was used to determine the product yield.

Single turnover experiment of Mb compound I with thioanisole was performed in a similar manner for that of HRP, except that the compound I was prepared by the addition of *m*CPBA in a 50 mM sodium acetate buffer, pH 5.0, at 277 K, followed by the reaction with thioanisole.

1 was prepared by the addition of a stoichiometric amount of *m*CPBA to a CH_2Cl_2 solution of Fe^{III}TMP(OH) (0.1 mM) at 223 K, and then a solution of thioanisole (10 equiv.) was added to the green solution. Immediate completion of the reaction was confirmed by observation of a brown solution and the mixture was then submitted to GC-MS analysis. The yield was determined based on SIM peak area ratio of the sulfoxide to that of internal standard (benzophenone).

Redox Potential of Substrates. The oxidation potentials of DMAs and sulfides were determined by cyclic voltammetric or by second harmonic AC voltammetric measurements (BAS 100W) in CH_3CN containing 2 mM sulfides and 100 mM Bu_4NPF_6 at rt. CV: voltage sweep 100 mV/s; SHACV: 50 Hz, 4 mV/s.

Addition of *p*-methylthioanisole to HRP-I (10 μM, pH 7.0, 298 K) gave a mixture of compound II (oxoferryl) and the resting ferric state (Figure 2.2.1). Compound II was further reduced to the resting state, consistent with the results by Dunford et al.[14] On the other hand, incorporation of 18-labeled oxygen into sulfoxides from the oxidant $H_2{}^{18}O_2$ as well as the moderate enantioselectivity indicates the occurrence of an oxygen atom transfer from HRP-I to sulfides.[15,16] These results are well explained if one assumes an electron transfer from sulfide to HRP-I in the protein cage followed by two competitive processes, i) oxygen rebound to afford the sulfoxide and ii) diffusion of a sulfenium radical from the protein cage to allow the observation of HRP-compound II as shown in Scheme 2.2.1.[14-17]

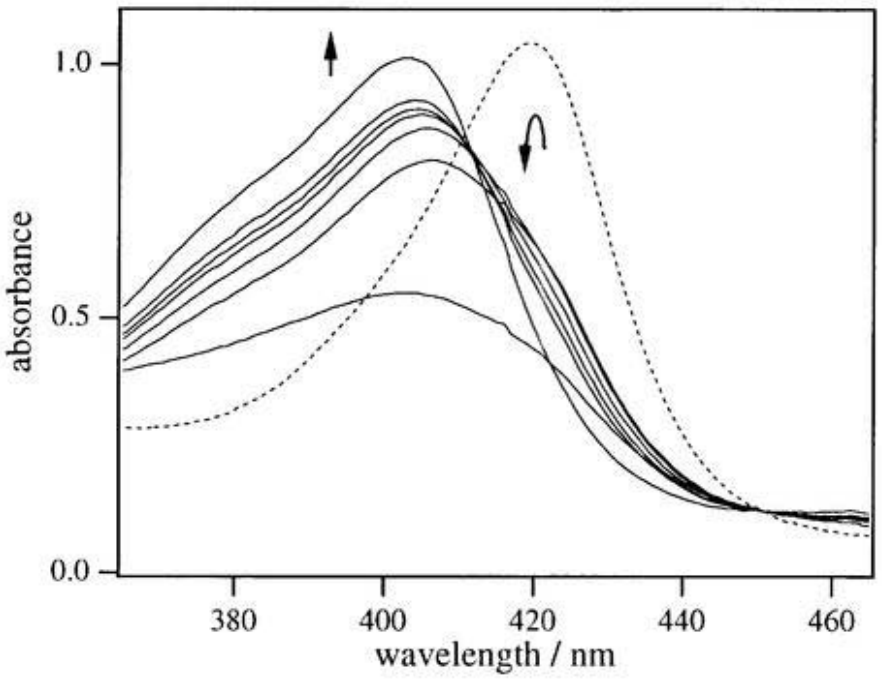

Figure 2.2.1. UV-vis spectral changes of the reaction of HRP-compound I with *p*-tolylmethyl sulfide in 50 mM sodium phosphate buffer, pH 7.0 at 298 K. [HRP] = 10 μM, [TolSMe] = 1.0 mM The dotted line represents the spectrum of HRP-compound II for a reference.

Scheme 2.2.1

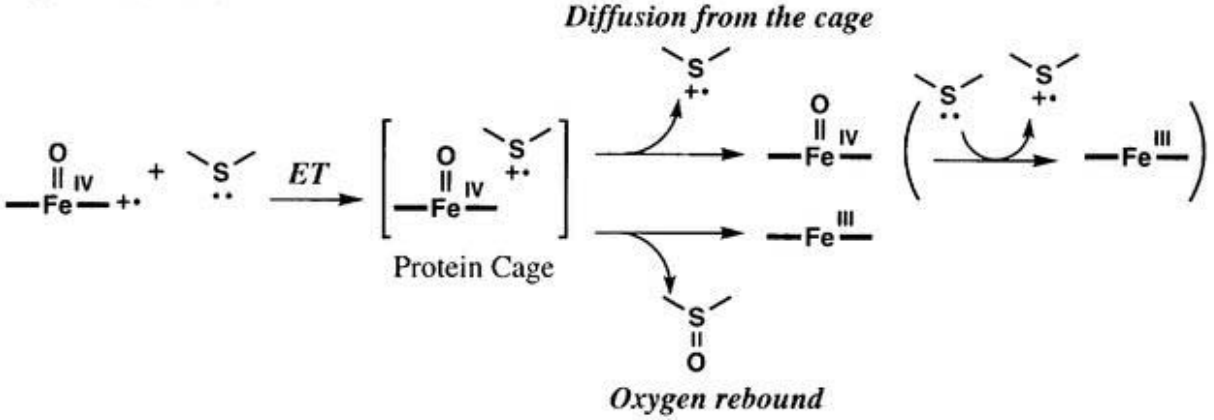

In order to estimate the efficiency of the oxygen-rebound step over the diffusion in Scheme 2.2.1, we have determined the yield of sulfoxide. The yield obtained from the stoichiometric reaction of HRP-I with thioanisole is only 25±5 %. The second-order rate constants (k_{obs}) for the reduction of HRP-I by a series of *p*-substituted thioanisoles in phosphate buffer (pH 7.0, 50 mM) at 298 K are summarized in Table 2.2.1. The log k_{obs} values are linearly correlated with the one-electron oxidation potentials of thioanisoles as shown in Figure 2.2.2(a) where the log k_{obs} values for electron transfer reactions from DMAs to HRP-I[10] are also included in a single linear correlation. Such a single correlation between log k_{obs} and E^0_{ox} together with the minor yield of sulfoxide indicates that the major pathway for the reduction of HRP-I by thioanisoles is sequential electron transfer rather than oxygen rebound.

The reaction of **1** with *p*-substituted thioanisoles in CH_2Cl_2 at 223 K monitored directly by a stopped-flow technique afforded Fe^{III}TMP without accumulation of any intermediates (Figure 2.2.3). The yield of methylphenyl sulfoxide by **1** was quantitative, indicating that the UV-vis spectral change corresponds to the oxygen transfer process. The second-order rate constants (k_{obs}) of the sulfoxidation by **1** were determined on the basis of the absorbance changes at 413 nm at 223 K. Figure 2.2.2.(b) shows a correlation between log k_{obs} for the sulfoxidation of thioanisoles by **1** and E^0_{ox} of

Table 2.2.1. Bimolecular Rate Constants of the Reactions of HRP-I, $O=Fe^{IV}TMP^{\bullet+}$ and H64S Mb-I with a Series of *p*-Substituted Thioanisoles and DTCO

Sulfide	E^0_{ox} vs SCE [V]	HRP k_{HRP} [$M^{-1}s^{-1}$]	TMPFe k_{TMP} [$M^{-1}s^{-1}$]	Mb H64S k_{Mb} [$M^{-1}s^{-1}$]
Thioanisoles				
p-OMe	1.13	$(8.4 \pm 0.1) \times 10^2$	$(1.7 \pm 0.1) \times 10^4$	$(1.2 \pm 0.1) \times 10^6$
p-Me	1.24	$(1.5 \pm 0.1) \times 10^2$	$(5.8 \pm 0.2) \times 10^3$	$(6.2 \pm 0.2) \times 10^5$
p-H	1.34	$(6.6 \pm 0.1) \times 10$	$(3.0 \pm 0.1) \times 10^3$	$(5.2 \pm 0.2) \times 10^5$
p-Cl	1.37	n.d.[a]	n.d.[a]	$(7.2 \pm 0.4) \times 10^5$
p-Br	1.41	n.d.[a]	$(2.4 \pm 0.1) \times 10^3$	$(5.2 \pm 0.1) \times 10^5$
p-CN	1.61	n.d.[a]	$(7.8 \pm 0.1) \times 10^2$	$(8.4 \pm 0.1) \times 10^4$
p-NO_2	1.70	n.d.[a]	$(5.1 \pm 0.1) \times 10^2$	n.d.[a]
DTCO	0.72	k_2: $(1.2 \pm 0.1) \times 10^3$ k_3: $(3.4 \pm 0.3) \times 10$ [b]	$(8.6 \pm 0.8) \times 10^3$	k_2: $(4.3 \pm 0.1) \times 10^5$ k_3: $(1.2 \pm 0.1) \times 10^3$ [b]

[a] Not determined. [b] k_2 and k_3 corresponds to the rate constant from compound I to compound II and from compound II to ferric, respectively.

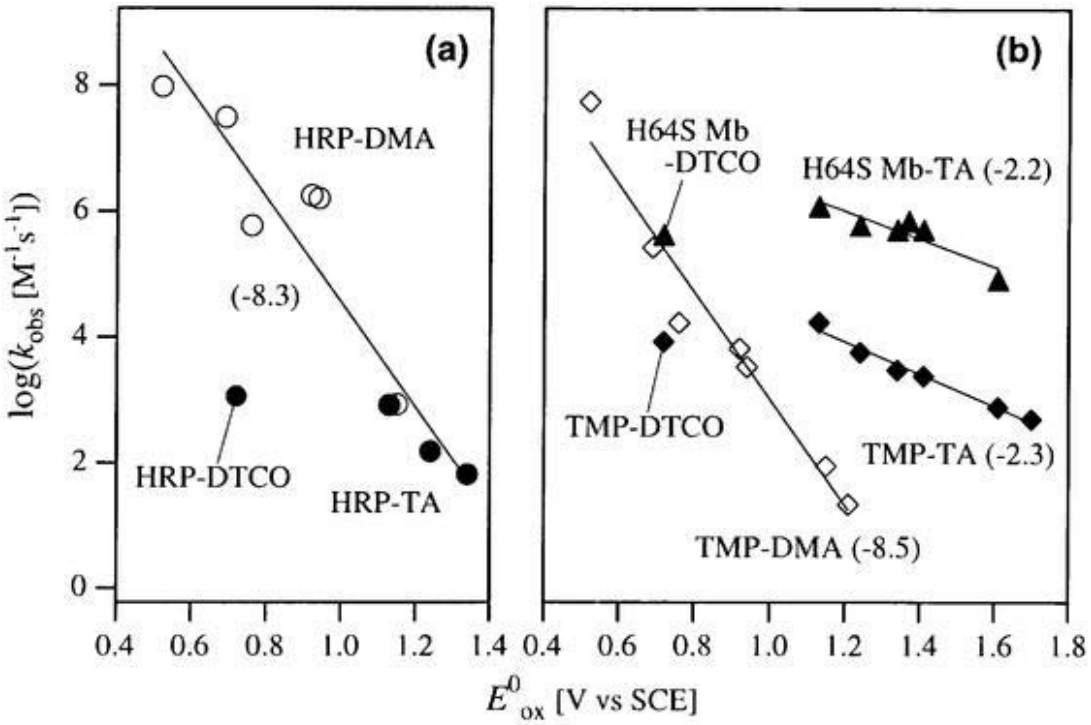

Figure 2.2.2. Dependence of rate constants on the oxidation potential of sulfides and DMAs (E^0_{ox}). TA: thioanisoles; DTCO: 1,5-dithiacyclooctane; DMA: N,N-dimethylaniline. The slopes of each line are shown in parentheses: (a) bimolecular rate constants of the reaction of ○) HRP-I with DMAs; ●) HRP-I with sulfides: (b) ◇) O=Fe^{IV}TMP$^{+\bullet}$ with DMAs; ◆) O=Fe^{IV}TMP$^{+\bullet}$ with sulfides; ▲) H64S Mb-compound I with sulfides.

thioanisoles in comparison with a linear correlation between log k_{obs} for the electron transfer from DMAs to **1** and E^0_{ox} of DMAs.[10] In contrast with the case of HRP-I in Figure 2.2.2(a), the k_{obs} values of thioanisoles in Figure 2.2.2(b) are at least two-orders of magnitude larger than those of electron transfer from DMAs to **1** when they are compared at the same E^0_{ox} values. This indicates that the reduction of **1** by thioanisoles proceeds via direct oxygen transfer rather than the electron transfer/oxygen rebound pathway shown in Scheme 2.2.1.

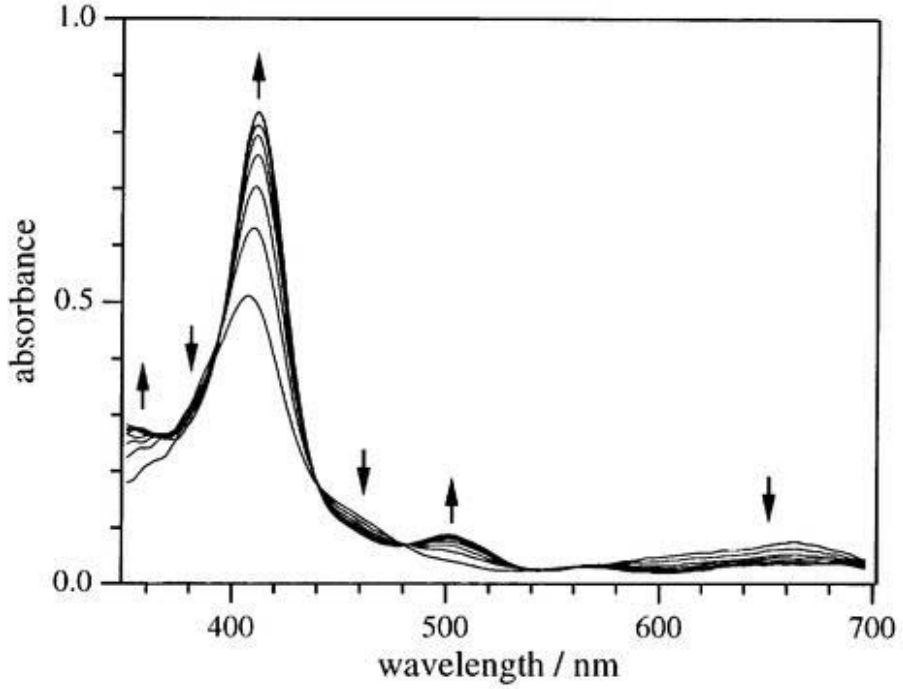

Figure 2.2.3. UV-vis spectral changes on the reaction of $O=Fe^{IV}TMP^{+\bullet}$ (5.0 μM) with thioanisole (400 μM) in CH_2Cl_2 at 223 K. The spectra were recorded for 880 (every 80) msec after mixing.

The reduction of H64S Mb-I by thioanisoles has also been examined, and the spectral changes for the reaction show direct reduction of the compound I by thioanisole to the ferric state with several isosbestic points (Figure 2.2.4),[11] accompanied by the formation of methylphenylsulfoxide in a quantitative yield. The second-order rate constants (k_{obs}) for the reduction of H64S Mb-I by thioanisoles were determined in acetate buffer (pH 5.0) at 277 K. The results are compared with those of **1** in Figure 2.2.2(b), where the log k_{obs} values are plotted against the E^0_{ox} values of thioanisoles. A parallel relationship between the plots of **1** and H64S Mb-I, both of which are far above the electron transfer correlation for the reduction of HRP-I by DMAs and thioanisoles, indicates that the reduction of H64S Mb-I also proceeds via direct oxygen transfer rather than the electron transfer/oxygen rebound pathway.

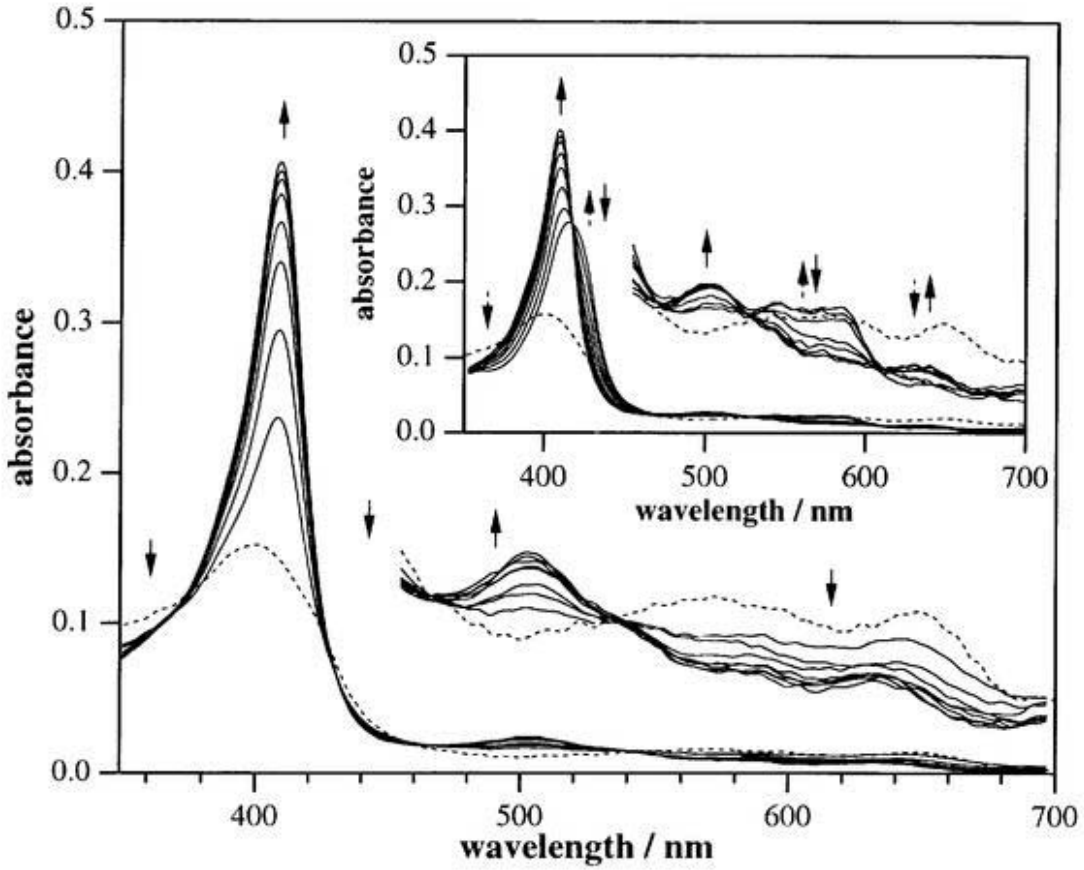

Figure 2.2.4. UV-vis spectral changes in the reaction of H64S Mb-I (2.5 μM) with thioanisole (100 mM) in 50 mM sodium acetate buffer, pH 5.0 at 277 K. The spectra were recorded for 84 msec after mixing. *Insets*: UV-vis spectral changes in the reaction of H64S Mb-I (2.5 μM) with DTCO (25 μM) in 50 mM sodium acetate buffer, pH 5.0 at 277 K. The spectra were recorded for 12.8 (every 1.6) sec after mixing. The dotted line is the spectrum before the reaction (i.e. the spectrum of H64S Mb-I).

When 1,5-dithiacyclooctane (DTCO), of which E^0_{ox} is much lower than those of thioanisoles[18], is employed as a substrate for the reduction of **1**, the k_{obs} value becomes even smaller than the value expected from the electron transfer correlation between log k_{obs} and E^0_{ox} in Figure 2.2.2(b). Such a smaller k_{obs} value of DTCO as compared with the k_{obs} value of DMAs at the same E^0_{ox} value is consistent with the larger reorganization energy (λ) expected for the electron transfer oxidation to produce a σ radical cation ($DTCO^{\bullet+}$) than the λ values of π radical cations ($DMAs^{\bullet+}$).[19] Thus, the reduction of **1**

by DTCO may proceed via electron transfer from DTCO to **1** (Figure 2.2.5). An alteration of the reaction mechanism from direct oxygen transfer to electron transfer becomes more evident in the reduction of H64S Mb-I by DTCO, i.e., rapid formation of compound II, $(4.3 \pm 0.1) \times 10^5\ M^{-1}\ s^{-1}$, followed by the slower reduction to the ferric state, $(1.2 \pm 0.1) \times 10^3\ M^{-1}\ s^{-1}$ (Table 2.2.1, Figure 2.2.4 *inset*).

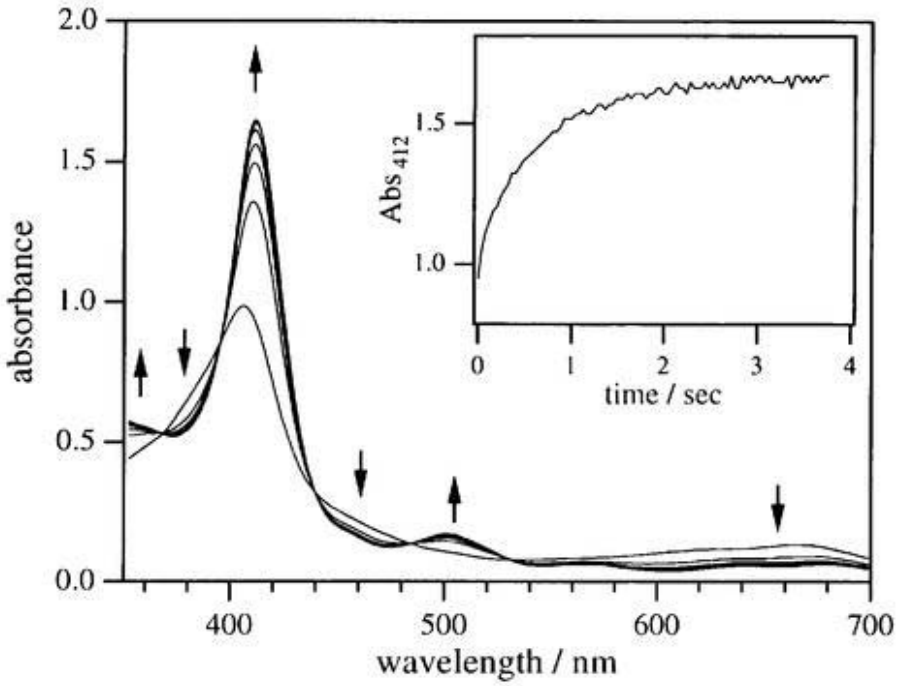

Figure 2.2.5. UV-vis spectral changes on the reaction of $O{=}Fe^{IV}TMP^{+\bullet}$ (10 μM) with 1,5-dithiacyclooctane (200 μM) in CH_2Cl_2 at 223 K. The spectra were recorded for 3.38 (every 0.46) sec after mixing. (inset) Time course absorbance change at 412 nm.

The P450 enzymes are known to mediate N- and O-demethylation (dealkylation) and S-oxidation (Table 2.2.2) in addition to hydroxylation and epoxidation. Watanabe et al. have suggested an electron transfer process for S-oxidation by $P450_{LM2}$ based on the following observations:[20,21] (1) the oxidation product of P450 is generally S-oxide; (2) S-dealkylation competes when sulfides bearing active α-hydrogens, such as phenyl-phenacylsulfide, were employed; (3) the extent of S-dealkylation increased with the

acidity of the α-hydrogens of the sulfide; (4) the dealkylation activity was depressed if sulfides having substituents that destabilize α-radical intermediates were employed. Scheme 2.2.2 summarizes these results. When the sulfenium radical was prepared by the reaction of the hydroxy radical and sulfides, the same product distribution as that observed in the P450 system was obtained.[20] Furthermore, kinetic studies of the enzymatic S-oxygenation of substituted thioanisoles showed correlation of V_{max} with the Brown-Okamoto σ^+ ($\rho = 0.61$),[21,22] whereas the oxidation by an electrophilic oxidant such as *m*CPBA gave only S-oxide, with relative rates that correlate with Hammett σ-values.[23] The oxidation of sulfides by a model porphyrin system, $Fe^{III}TPP/H_2O_2$/imidazole, showed similar reactivity (Table 2.2.2).[24-26]

Table 2.2.2.[27] Ratios between S-Oxidation and S-dealkylation in oxidation of phenylphenacylsulfide with various oxidants

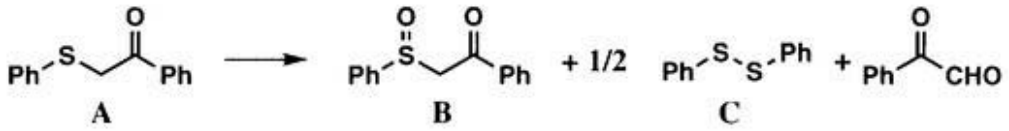

Oxidation System	Solvent	Ratio (B:C)
P450/NADPH/O_2	Buffer (pH 7.4)	48 : 52
$Fe^{III}TPP/H_2O_2$/imidazole	CH_3CN	86 : 14
$Fe^{II}(ClO_4)_2/H_2O_2$	Methanol	49 : 51
FAD-monooxygenase/NADPH/O_2	Buffer (pH 7.4)	100 : 0
4a-FlEt-OOH	Dioxane	100 : 0
*m*CPBA	CH_2Cl_2	100 : 0
H_2O_2	Acetic acid	100 : 0

Correlations of reaction rates with oxidation potentials, however, particularly when based on a very limited number of compounds, are suggestive but do not require enzymatic oxidation of sulfur to a radical cation because two-electron oxidation mechanisms also depend on the substrate oxidation potentials. An example of the

coincidence of substituent effects for one- and two-electron oxidation mechanisms is provided by work on the chemical oxidation of NAD (nicotinamide dinucleotide) analogues.[28] The oxidation of phenyl cyclopropyl sulfide by the fungus *Mortierella isabellina* has been investigated in the hope that cyclopropyl ring opening would evidence for a sulfur radical cation intermediate.[29] However, sulfoxidation occurred without detectable opening of the cyclopropane ring.

Though we have observed that the compounds I of HRP, H64S Mb, and FeTMP complex oxidize a sulfide, DTCO, bearing low redox potential, through electron transfer, compounds I of H64S Mb and FeTMP oxidize thioanisole by the mechanism which does not involve one-electron transfer/oxygen rebound process. If this is the case even for P450-catalyzed sulfoxidation, there must be a transient intermediate which allows competitive process for the S-dealkylation. One of possible intermediates could be sulfenium cation as shown below in Scheme 2.2.2.

Scheme 2.2.2

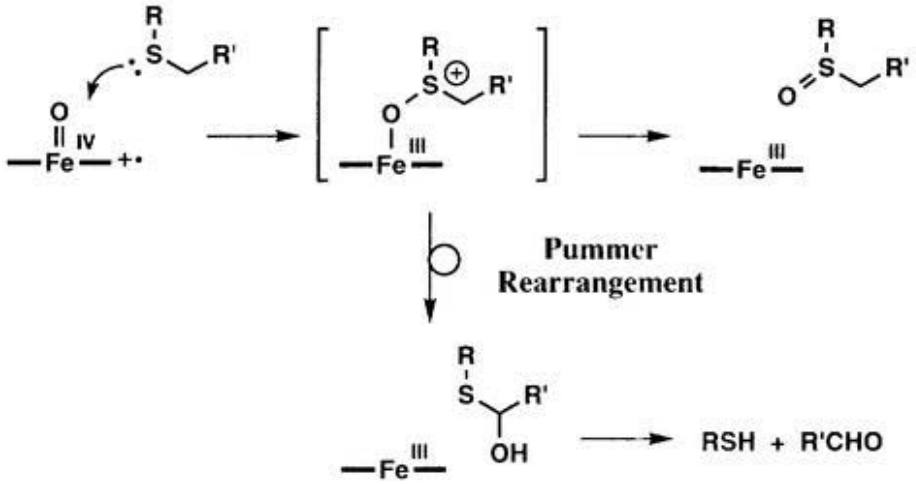

In conclusion, the reaction of HRP-compound I by thioanisoles proceeds via electron transfer, while the sulfoxidation of thioanisoles with **1** and H64S Mb-compound I occurs via direct oxygen transfer. When thioanisoles are replaced by a much stronger reductant (e.g. DTCO), however, the sulfoxidation proceeds via electron transfer.

REFERENCE

(1) Ortiz de Montellano, P. R. *Cytochrome P450. Structure, Mechanism, and Biochemistry.;* 2nd ed.; Plenum Publishing Corporation: New York, 1995.

(2) Egawa, T.; Shimada, H.; Ishimura, Y. *Biochem. Biophys. Res. Commun.* **1994**, *201*, 1464-1469.

(3) Dunford, H. B.; Stillman, J. S. *Coord. Chem. Rev.* **1987**, *19*, 187-251.

(4) Harris, R. Z.; Newmyer, S. L.; Ortiz de Montellano, P. R. *J. Biol. Chem.* **1993**, *268*, 1637-1645.

(5) Newmyer, S. L.; Ortiz de Montellano, P. R. *J. Biol. Chem.* **1995**, *270*, 19430-19438.

(6) Ozaki, S.; Ortiz de Montellano, P. R. *J. Am. Chem. Soc.* **1995**, *117*, 7056-7064.

(7) Savenkova, M. I.; Kuo, J. M.; Ortiz de Montellano, P. R. *Biochemistry* **1998**, *37*, 10828-36.

(8) Watanabe, Y. In *Oxygenase and Model Systems*; T. Funabiki, Ed.; Kluwer Academic Publishers: Dordrecht, The Netherland, 1997; pp 223-282.

(9) Groves, J. T.; Watanabe, Y. *J. Am. Chem. Soc.* **1988**, *110*, 8443-8452.

(10) Goto, Y.; Watanabe, Y.; Fukuzumi, S.; Jones, J. P.; Dinnocenzo, J. P. *J. Am. Chem. Soc.* **1998**, *120*, 10762-10763.

(11) Matsui, T.; Ozaki, S.; Watanabe, Y. *J. Biol. Chem.* **1997**, *272*, 32735-32738.

(12) Ozaki, S.; Matsui, T.; Watanabe, Y. *J. Am. Chem. Soc.* **1997**, *119*, 6666-6667.

(13) Ozaki, S.; Matsui, T.; Watanabe, Y. *J. Am. Chem. Soc.* **1996**, *118*, 9784-9785.

(14) Perez, U.; Dunford, H. B. *Biochemistry* **1990**, *29*, 2757-2763.

(15) Doerge, D. R.; Cooray, N. M.; Brewster, M. E. *Biochemistry* **1991**, *30*, 8960-4.

(16) Kobayashi, S.; Nakano, M.; Goto, T.; Kimura, T.; Schaap, A. P. *Biochem. Biophys. Res. Commun.* **1986**, *135*, 166-171.

(17) Perez, U.; Dunford, H. B. *Biochim. Biophys. Acta.* **1990**, *1038*, 98-104.

(18) Wilson, G. S.; Swanson, D. D.; Klug, J. T.; Glass, R. S.; Ryan, M. D.; Musker, W. K. *J. Am. Chem. Soc.* **1979**, *101*, 1040-1042.

(19) Eberson, L. *Electron Transfer Reactions in Organic Chemistry*; Springer-Verlag: Berlin, 1987.

(20) Watanabe, Y.; Numata, T.; Iyanagi, T.; Oae, S. *Bull. Chem. Soc. Jpn.* **1981**, *54*, 1163.

(21) Watanabe, Y.; Iyanagi, T.; Oae, S. *Tetrahedron Lett.* **1980**, *21*, 3685.

(22) Watanabe, Y.; Iyanagi, T.; Oae, S. *Tetrahedron Lett.* **1982**, *23*, 533.

(23) Modena, G.; Mariola, L. *Gazz. Chim. Ital.* **1957**, *87*, 1306.

(24) Oae, S.; Watanabe, Y.; Fujimori, K. *Tetrahedron Lett.* **1982**, *23*, 1189.

(25) Oae, S.; Fujimori, K. *J. Synth. Org. Chem. Jpn.* **1983**, *41*, 848.

(26) Asada, K. MS Thesis, University of Tsukuba, 1983.

(27) Watanabe, Y.; Groves, J. T. In *The Enzymes*; P. D. Boyer and D. S. Sigman, Ed.; Academic Press: New York, 1992; Vol. 20; pp 405-452.

(28) Powell, M. F.; Wu, J. C.; Bruice, T. C. *J. Am. Chem. Soc.* **1984**, *106*, 3850-3856.

(29) Holland, H. L.; Chernishenko, M. J.; Conn, M.; Munoz, A.; Manoharan, T. S.; Zawadski, M. A. *Can. J. Chem.* **1990**, *68*, 696-700.

CHAPTER 3

Structure-Mechanism Relationships of Heme Enzymes

ABSTRACT: The sperm whale myoglobin His64Ser mutant gives a relatively stable oxoferryl porphyrin π-cation radical intermediate equivalent to so-called compound I intermediate of peroxidases, upon the addition of a stoichiometric amount of *m*CPBA (Matsui et al., *J. Biol. Chem.* 1997). Oxidations of a series of N,N-dimethylanilines (DMAs), thioanisoles and styrenes by His64Ser Mb-compound I have been directly observed by employing a rapid-scan stopped-flow UV-vis spectroscopy. In the reaction with DMAs, the His64Ser Mb-compound I was reduced to the ferric state via compound II which is a one-electron reduced form of compound I, while the direct 2-electron process coupled with oxygen transfer was observed in the reactions with thioanisoles and styrenes. The second-order rate constants for the reactions of His64Ser Mb-compound I with the DMAs are independent of the one-electron oxidation potentials of DMAs in contrast to the cases of horseradish peroxidase (HRP) and its synthetic model complex, TMPFe (TMP = 5,10,15,20-tetramesitylporphine dianion). This is presumably due to the substrate binding being the rate-limiting step in the case of His64Ser Mb. On the contrary, the reaction profile of sulfoxidation of thioanisoles by His64Ser Mb-compound I was similar to the case of TMPFe, indicating the direct oxygen transfer mechanism (Chapter 2). Styrene oxidation by His64Ser Mb-compound I showed a similar reaction profile to that of thioanisole sulfoxidation, implying direct oxygen transfer. However, the α-methylstyrene oxidation rate is slower than that of styrene by one order of magnitude. This provides information on structure-mechanism relationship of His64Ser Mb mutant.

ABBREVIATIONS

compound I	an oxoferryl porphyrin π-cation radical
compound II	an oxoferryl porphyrin
HRP	horseradish peroxidase
Mb	myoglobin
TMP	5,10,15,20-tetramesitylporphine dianion

*m*CPBA	3-chloroperbenzoic acid
TA	thioanisole
DMA	N,N-dimethylaniline
DTCO	1,5-dithiacyclooctane
CV	cyclic voltammetry
SHACV	second harmonic AC voltammetry

2.3.1 INTRODUCTION

Cytochrome P450 catalyzes oxygenation of organic compounds efficiently,[1,2] however, oxygenation mechanisms are poorly understood mainly because the reactive intermediate of cytochrome P450 have not yet been observed.[3] Although an oxoferryl porphyrin π-cation radical equivalent to so-called compound I in peroxidases[4] has been postulated as a reactive intermediate of cytochrome P450, the mechanistic features and the reactivity of compound I of cytochrome P450 are still ambiguous. In chapter 2, we have succeeded a direct observation of the sulfoxidation by compound I of HRP,[5,6] a synthetic porphyrin complex and the sperm whale myoglobin H64S mutant.[7] Through the kinetic studies, the sulfoxidation of thioanisole by HRP-compound I has been found to proceed via electron transfers in good accordance with its native function. In contrast, the synthetic model and H64S Mb mutant exhibit sulfoxidation via the direct oxygen transfer.[7]

It is surprising that H64S Mb-compound I exhibits different reactivities from those of HRP, because of the expectation that the active site structure of H64S Mb would be similar to that of HRP. The oxygen transfer ability of H64S Mb-compound I prompts us to use this species as a protein model for compound I of cytochrome P450 to investigate the detailed reactivities and mechanisms of oxygenations.

In this Chapter, we have examined N-demethylation of N,N-dimethylaniline derivatives and epoxidation of a series of styrenes by H64S Mb-compound I to clarify the nature of Mb-compound I. The structure-mechanism relationship of the Mb mutant is also discussed based on the reactivities of styrenes bearing different structural features, together with a comparison of X-ray crystal structures of HRP[8], P450[9] and H64S Mb mutant[10].

2.3.2 EXPERIMENTAL PROCEDURE

Chemicals. All chemicals were purchased from Sigma-Aldrich, Wako, Nacalai tesque and Lancaster Co., Ltd. and used without further purification unless otherwise

noted. *m*CPBA was purified by washing its dichloromethane solution with phosphate buffer (pH 7.4) followed by water and then dried under reduced pressure. N,N-dimethyl-*p*-toluidine and N,N-dimethylaniline were purified by distillation and stored under Ar atmosphere until use. The other *p*-substituted N,N-dimethylanilines including D-labeled compounds were prepared by a method previously reported.[11] Styrene derivatives were distilled by a Kügel Rhor to remove the stabilizer, 3,5-di-*tert*-butylcatecol, prior to use.

Myoglobin Mutant. Sperm whale myoglobin His64Ser mutant was constructed by cassette mutagenesis. The expression vector for wild type of sperm whale myoglobin is a gift from Professor Olson (Rice University).[7,12]

Kinetic Experiments. Kinetic experiments for the oxidation of N,N-dimethylanilines and styrenes by H64S Mb-compound I were performed with a Hi-Tech SF-43 stopped-flow apparatus equipped with a MG 6000 diode array spectrophotometer for rapid-scan UV-vis spectroscopic measurements and with a MG 60 photomultiplier for singlewavelength measurements. H64S Mb-compound I was prepared by mixing H64S Mb (10 μM) with 1.5 equiv of *m*CPBA followed by mixing with a N,N-dimethylaniline or styrene derivative at 277 K in 50 mM sodium acetate buffer (pH 5.0) with a double-mixing mode (delay time: 2.1 sec, final concentration of Mb: 2.5 μM). The amount of substrate was kept 10-500 equivalents over Mb for ensuring the pseudo-first-order condition. Solutions of substrates for kinetic measurements were prepared by dilution of a stock solution of substrates in MeOH (10-40 mM) with the acetate buffer. The rates of N,N-dimethylaniline oxidation by H64S Mb-compound I were determined by fitting the change in absorbance at 418 and 408 nm (*see also RESULTS*). The rates of the styrene oxidation were determined by fitting the change in absorbance at 408 nm with a least-squares procedure. The pseudo-first-order rate constants are proportional to the substrate concentration, thus, the second-order rate constants were determined by the slope.

Redox Potential of Substrates. The oxidation potentials of DMAs were determined by cyclic voltammetric measurements as described in Chapter 1 of this Part.[13] Irreversible cyclic voltammograms were obtained for styrenes, thus, the oxidation

potentials (E^0_{ox}) of styrene, α-methylstyrene, *trans*- and *cis*-β-methylstyrene were determined by second harmonic AC voltammetry (SHACV, BAS 100W) with 50 Hz, voltage sweep 4 mV/s. E^0_{ox} of the other *p*-substituted styrenes were estimated on the bases of peak potentials of styrene by CV and that by SHACV measurement.

RESULTS

Reactions of H64S Mb-Compound I and N,N-Dimethylanilines. Time-dependent UV-vis spectral changes in the reaction of H64S Mb-compound I with DMA are shown in Figure 2.3.1. Upon the addition of DMA, the compound I species

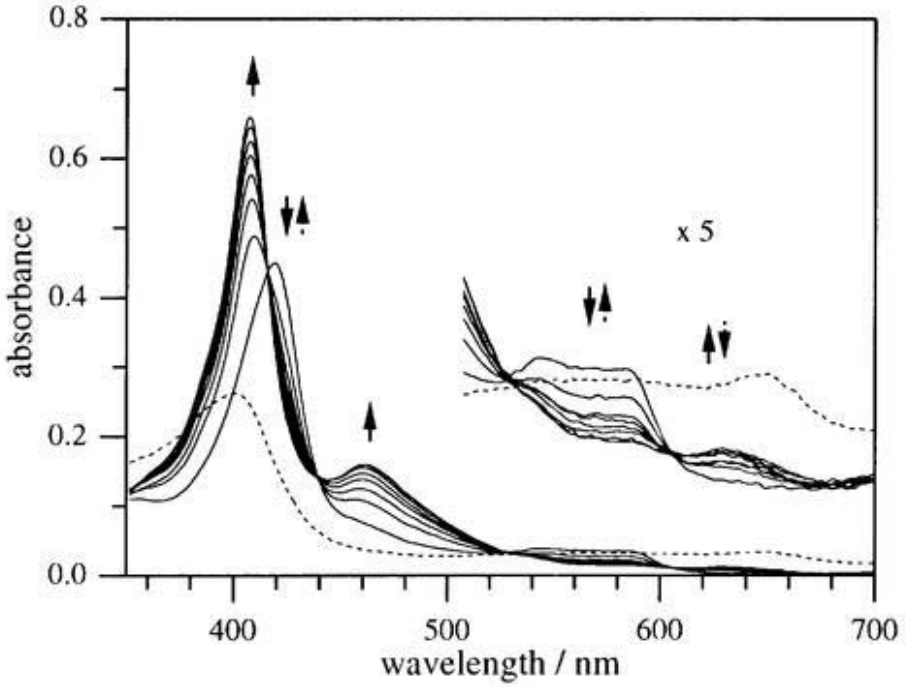

Figure 2.3.1. UV-vis spectral changes in the reaction of H64S Mb-compound I (5.0 μM) with thioanisole (50 μM) in 50 mM sodium acetate buffer, pH 5.0 at 277K. The spectra were recorded every 0.24 sec to 1.68 sec after the mixing. The dotted line indicates the spectrum before the reaction (H64S Mb-compound I).

was immediately reduced to compound II followed by a further reduction to the ferric resting state. Pseudo-first-order rate constants for the processes from compound I to compound II (k_{1app}) and compound II to ferric (k_{2app}) were determined on the basis of

changes in absorbance at 418 nm (an isosbestic point of Mb compound I and II) and at 399 nm, respectively. Both plots for k_{1app} and k_{2app} vs [DMA] are linearly-dependent (Figure 2.3.2). The second-order rate constants for each process in the reaction with a series of *p*-substituted DMAs are summarized in Table 2.3.1 together with the one electron oxidation potentials of DMAs (E^0_{ox}). The rate constants for the reactions of the mutant compound I with N,N-di(trideuteriomethyl)anilines were also determined, and the kinetic isotope effects are summarized in Table 2.3.1. No kinetic isotope effects are evident in all of the processes.

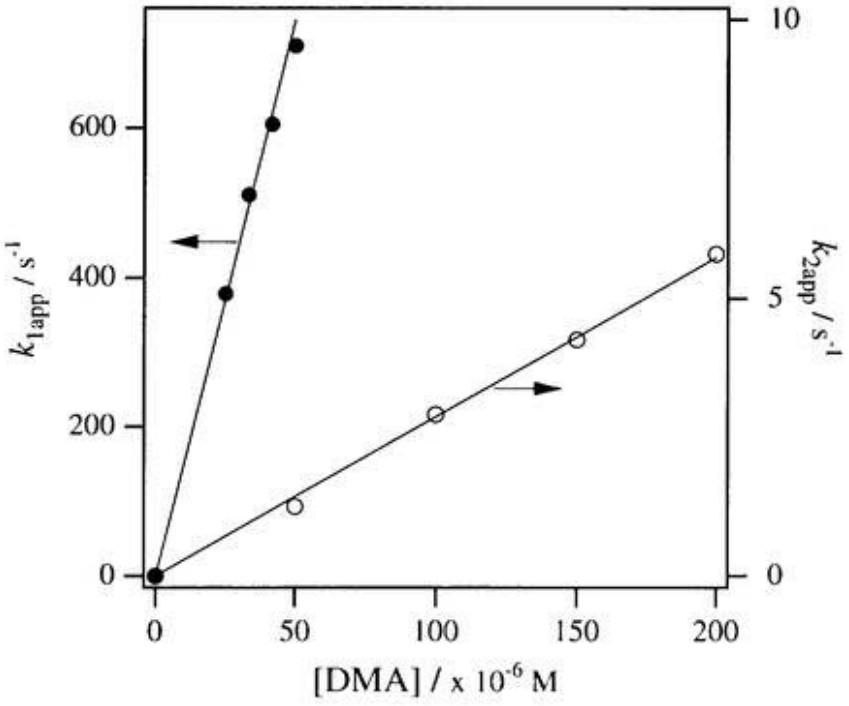

Figure 2.3.2. Plots of pseudo-first-order rate constants k_{1app} and k_{2app} vs [DMA] in the reaction of H64S Mb-compound I with DMA in 50 mM sodium acetate buffer, pH 5.0 at 277K. [H64S Mb-compound I] = 2.5 μM.

Table 2.3.1. Bimolecular Rate Constants and Kinetic Isotope Effects on the Reaction of Sperm Whale Myoglobin H64S Mutant Compounds I and II with a Series of *p*-Substituted DMA

p-substituent	$E_{1/2}$ [V vs Fc]	k_{1H} [$M^{-1}s^{-1}$]	k_{1H}/k_{1D}	k_{2H} [$M^{-1}s^{-1}$]	k_{2H}/k_{2D}
OMe	0.14	$(1.7 \pm 0.1) \times 10^7$	1.0 ± 0.1	$(1.8 \pm 0.1) \times 10^4$	1.0 ± 0.1
Me	0.33	$(1.7 \pm 0.1) \times 10^7$	1.1 ± 0.1	$(2.9 \pm 0.1) \times 10^4$	1.2 ± 0.1
H	0.53 [a]	$(1.5 \pm 0.1) \times 10^7$	1.0 ± 0.1	$(2.9 \pm 0.1) \times 10^4$	1.0 ± 0.1
Cl	0.50	$(3 \pm 1) \times 10^8$	n.d.[b]	$(1.6 \pm 0.1) \times 10^5$	0.9 ± 0.1
Br	0.47	$(2 \pm 1) \times 10^8$	n.d.[b]	$(1.7 \pm 0.1) \times 10^5$	1.1 ± 0.1
CN	0.82	$(1.6 \pm 0.1) \times 10^6$	1.0 ± 0.1	$(3.0 \pm 0.1) \times 10^4$	1.1 ± 0.1

[a] no reversible wave was detected CV measurements. [b] not determined.

Reactions of H64S Mb-Compound I with Styrenes. UV-vis spectral changes according to the reaction of H64S Mb-compound I with α-methylstyrene[7] at 277 K (pH 5.0) are shown in Figure 2.3.3. A two-electron process (i.e. the direct reduction of compound I to the ferric state by α-methylstyrene) is observed with several isosbestic points. The pseudo-first-order rate constants determined by change in absorbance at 408 nm show a linear-dependence on styrene concentration. The rate constants of the reactions with a series of styrenes are summarized in Table 2.3.2 with one-electron oxidation potentials of styrenes (E^0_{ox}).

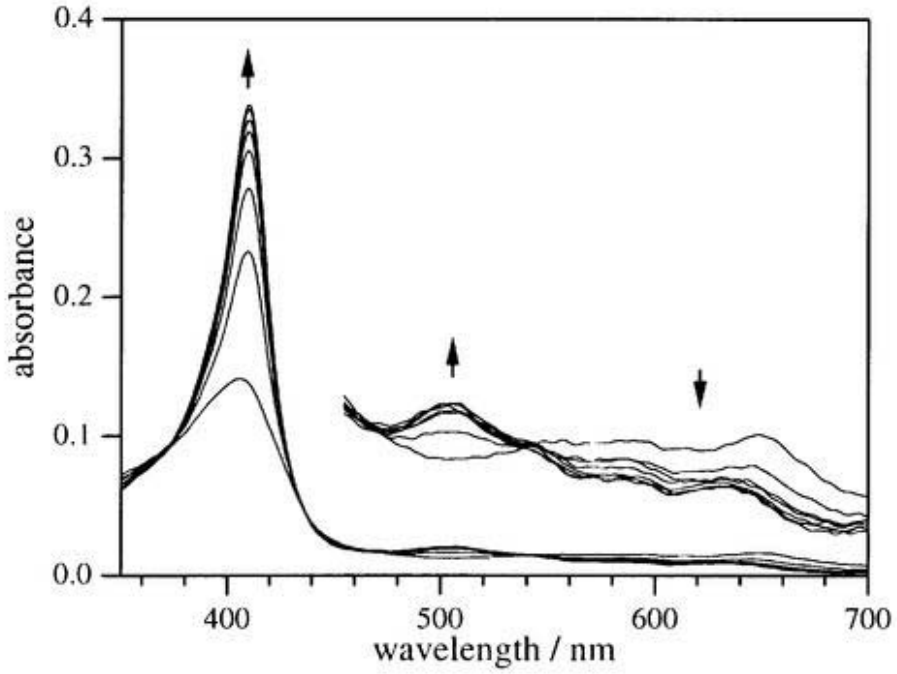

Figure 2.3.3. UV-vis spectral changes in the reaction of H64S Mb-compound I (2.5 μM) with α-methylstyrene (500 μM) in 50 mM sodium acetate buffer, pH 5.0 at 277K. The spectra were recorded at every 0.12 sec to 0.84 sec after mixing.

Table 2.3.2. Bimolecular Rate Constants of the Reactions of H64S Mb-compound I with a Series of *p*-Substituted styrenes

styrene	E^0_{ox} [V vs SCE][a]	k_{obs} [$M^{-1}s^{-1}$]
p-MeO	1.20	$(1.3 \pm 0.1) \times 10^5$
p-Me	1.63	$(2.4 \pm 0.5) \times 10^4$
p-H	1.95	$(2.0 \pm 0.1) \times 10^4$
p-Cl	1.91	$(3.8 \pm 0.1) \times 10^4$
α-Me	1.79	$(3.5 \pm 0.1) \times 10^3$
trans-β-Me	1.66	$(3.3 \pm 0.1) \times 10^5$
cis-β-Me	1.60	$(3.4 \pm 0.1) \times 10^4$

[a] In CH_3CN. Determined by SHACV measurements. [b] Fukuzumi, S. Personal communication. [c] Determined by CV then estimated by comparison with SHACV. See experimental section.

DISCUSSION

Reactions of H64S Mb-Compound I with DMAs. The UV-vis spectral changes in the reactions of H64S Mb-compound I with DMAs at 277 K in acetate buffer (pH 5.0) apparently exhibit sequential one-electron transfer from DMAs to compound I and then to compound II (Figure 2.3.1). The linear relationship between the pseudo-first-order rate constants for both steps and concentration of DMAs as well as a failure to observe kinetic isotope effect indicates that one-electron transfer processes occur between compound I or compound II and DMAs to afford a substrate cation radical (Table 2.3.1 and Figure 2.3.2). However, the rate constants are independent of the one-electron oxidation potentials of DMAs. This is very different from the typical electron transfer reactions observed for the N-demethylation of DMAs by HRP-compounds I and II (Figure 2.3.4).[13] These kinetic profiles can be explained if one assumes the rate-limiting step of the reaction to be a substrate binding step. If this is the case, electron transfer

rates are much greater than k_1 and k_2 listed in Table 2.3.1, implying the redox potential of compound I and compound II of the Mb mutant must be higher than those of HRP, since the k_1 and k_2 values for the Mb mutant are comparable to those of HRP (Figure 2.3.3).

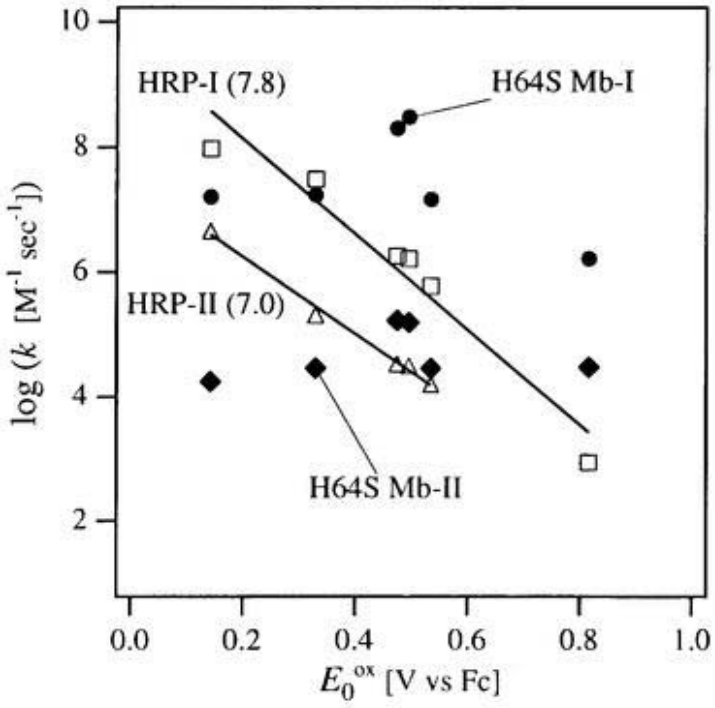

Figure 2.3.4. Dependence of rate constants on the oxidation potential of DMAs (E^0_{ox}): ●) H64S Mb-compound I; ◆) H64S Mb-compound II; □) HRP-compound I; △) HRP-compound II. The slopes of each line are shown in parentheses.

As described in the previous chapter, H64S Mb-compound I oxidizes thioanisole derivatives by direct oxygen transfer rather than the mechanism which involves an electron transfer process. Thus, the Mb mutant carries out both peroxidase (sequential one electron oxidation) and peroxygenase (oxygen transfer) activities, depending on the substrates employed.

Oxidation of styrenes by H64S Mb-compound I. The spectral changes observed for the reactions of H64S Mb-compound I with styrenes exhibit two-electron

reduction of compound I to the ferric state without accumulation of any intermediates. This result is similar to that observed for the reactions with thioanisoles (Figure 2.3.3). The plot of the logarithm of the rate constants of the reactions *vs* one-electron oxidation potentials of substrates (E^0_{ox}) in Figure 2.3.5. show linear correlation with E^0_{ox}, however, substituent effect is much smaller than that expected for an electron transfer process from the substrate to H64S Mb-compound I, but rather similar to that observed for the direct oxygen transfer to thioanisoles (see Chapter 2, PART II).[14] On the basis of these considerations, epoxidation of styrene by compound I of Mb is concluded to proceed via direct oxygen transfer.

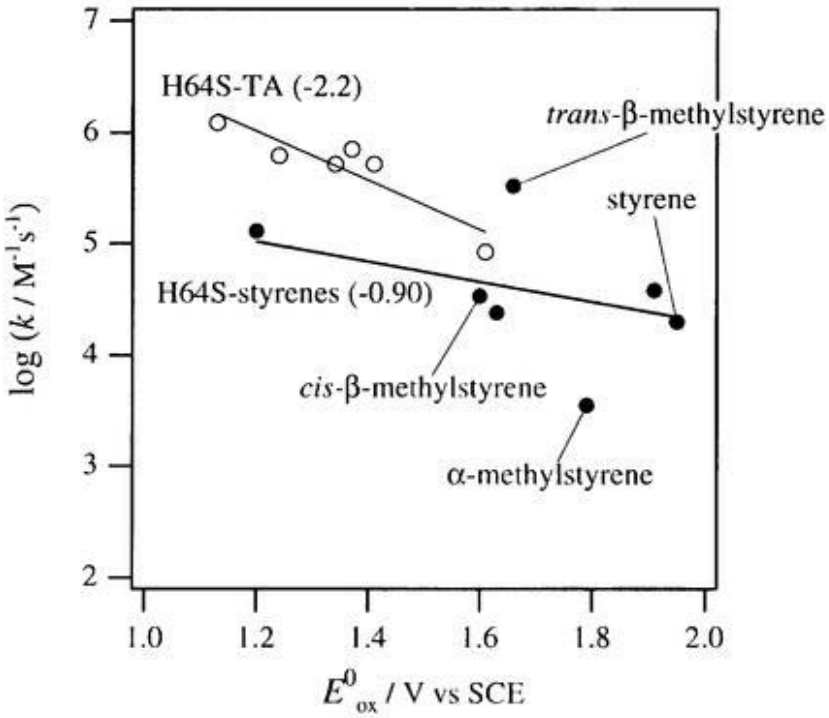

Figure 2.3.5. Dependence of rate constants on the oxidation potential of thioanisoles and styrenes (E^0_{ox}): Bimolecular rate constants of reaction of O) H64S Mb-compound I with thioanisoles; ●) H64S Mb-compound I with styrenes. The slopes of lines are shown in parentheses.

On the other hand, α-methylstyrene seems to be out of the linear correlation and the rate constant of 3.5×10^3 $M^{-1}s^{-1}$ is one order of magnitude lower than that of styrene (2.0×10^4 $M^{-1}s^{-1}$) even though the E^0_{ox} is ~160 mV lower than that of styrene (Table 2.3.2).[15] A similar decrease of the rate is also observed in the *trans*- and *cis*-β-methylstyrene. The one-electron oxidation potential of *cis*-β-methylstyrene is comparable to that of *trans* isomer, though the rate constant for the *cis* isomer is smaller by one order over the *trans* isomer (Table 2.3.2).[15] As expected from Figure 2.3.5, the oxidation rate of *cis*-β-methylstyrene is on the line of styrenes. The decrease of the rates for these styrene derivatives could be attributed to the steric effect of heme vicinity as depicted in Scheme 2.3.1.

Structure-Mechanism Relationships of HRP, H64S Mb mutant and P450. As described in the previous and present chapter, compounds I of HRP, H64S Mb and a synthetic model, $O=Fe^{IV}TMP^{+\bullet}$,[16] oxidize DMAs via electron transfer.[13] HRP-compound I also carries out the sequential one-electron oxidation of thioanisoles.[5,6,17,18] On the other hand, H64S Mb-compound I and $O=Fe^{IV}TMP^{+\bullet}$ oxidize thioanisoles by the direct oxygen transfer process rather than electron transfer. Thus, the sulfoxidation proceeds almost quantitative in the latter systems while HRP-compound I affords a small amount of sulfoxide.[19,20] Only the exception is the oxidation of dithiacyclooctane,[21] which shows very low redox potential, by H64S Mb-compound I. These differences in reactivity of three types of compound I species can be considered in connection with the structures of heme vicinity.[22-24] Figure 2.3.6 shows an X-ray crystal structure of heme vicinity of HRP.[8] As pointed out by Ortiz de Montellano and his co-workers, on the basis of phenyl- and alkylhydrazine ligation to the heme irons of various heme proteins, the heme of HRP is sheltered or surrounded by protein side chains which prevent easy-access of external molecules to the oxo ligand of compound I.[12,25] Thus, HRP-compound I prefers a sequential electron transfer over the oxygen transfer reaction. At the same time, substrate cation radicals formed by one-electron transfer in the active site are unable to accept the oxo ligand on the heme iron due to steric

Scheme 2.3.1

(1.41 V)

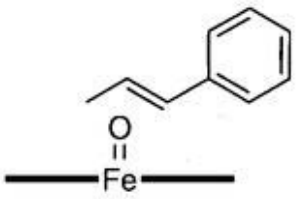

$k = 3.3 \times 10^5\ M^{-1}s^{-1}$

(1.41 V)

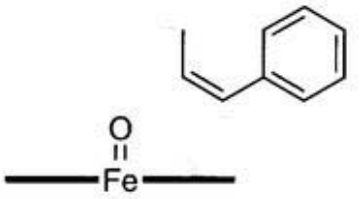

$k = 3.4 \times 10^4\ M^{-1}s^{-1}$

(1.88 V)

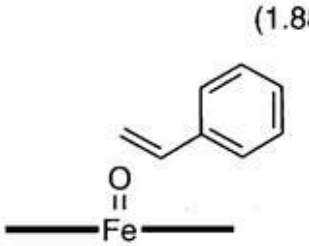

$k = 2.0 \times 10^4\ M^{-1}s^{-1}$

(1.82 V)

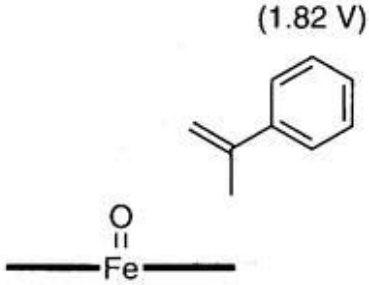

$k = 3.5 \times 10^3\ M^{-1}s^{-1}$

(1.13 V)

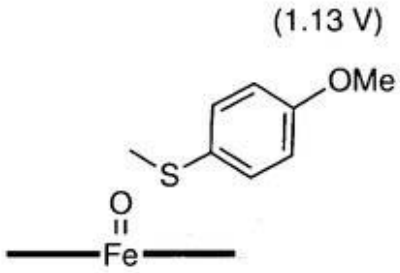

Oxygen Transfer

(1.15 V)

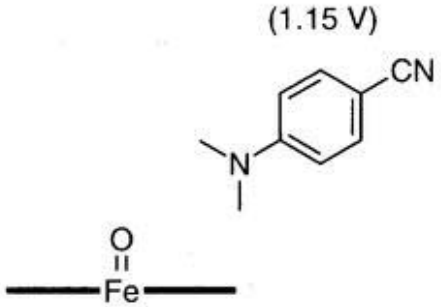

Electron Transfer

hindrance.[8] Consequently, the substrate cation radicals readily diffuse out of the active site (Scheme 2.3.2). This might be the reason why HRP-compound II is observable in the course of substrate oxidations.

Scheme 2.3.2

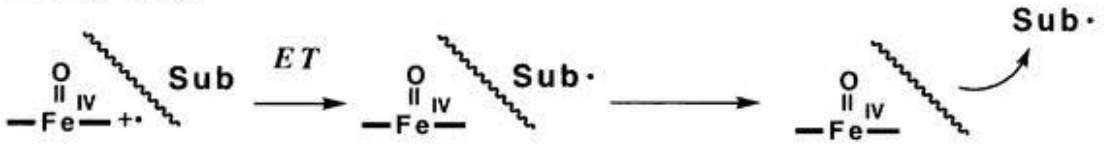

On the contrary, most of substrates are able to access to the O=Fe moiety of $O=Fe^{IV}TMP^{+\bullet}$ in a homogeneous organic solvent without any steric hindrance. Thus, the synthetic model porphyrin complex never gives compound II in the oxidation even though DMA oxidation proceeds via one-electron transfer, since the formed substrate cation radical readily reacts with $O=Fe^{IV}TMP$, one electron reduced state from $O=Fe^{IV}TMP^{+\bullet}$, in the solvent cage. In addition, the direct oxygen transfer becomes a favorable process if electron transfer is slower, (i.e., in the oxidation of substrates whose redox potentials are much higher than those of DMAs). The rate of electron transfer decreases, and the direct reaction of substrates with the oxygen bound to the heme iron of compound I becomes much faster than electron transfer if the substrate is able to freely access the active site. This could be the reason why $O=Fe^{IV}TMP^{+\bullet}$ oxidizes substrates by two different mechanisms which are dependent on the redox potential of the substrate.

The H64S Mb mutant has a relatively open heme environment compared to HRP. The substrate is thus able to easily access the oxo ligand of compound I, as suggested by the X-ray crystal structure of His64Thr Mb shown in Figure 2.3.7.[10] Therefore, the mechanistic features of substrate oxidations are quite similar to those of the model systems. However, bulkiness of the substrate sensitively affects the reaction rate of styrene oxidation by H64S Mb-compound I. Addition of α-methyl group to styrene or structural change from *trans*- to *cis*-β-methylstyrene reduces the rate of the oxidations by

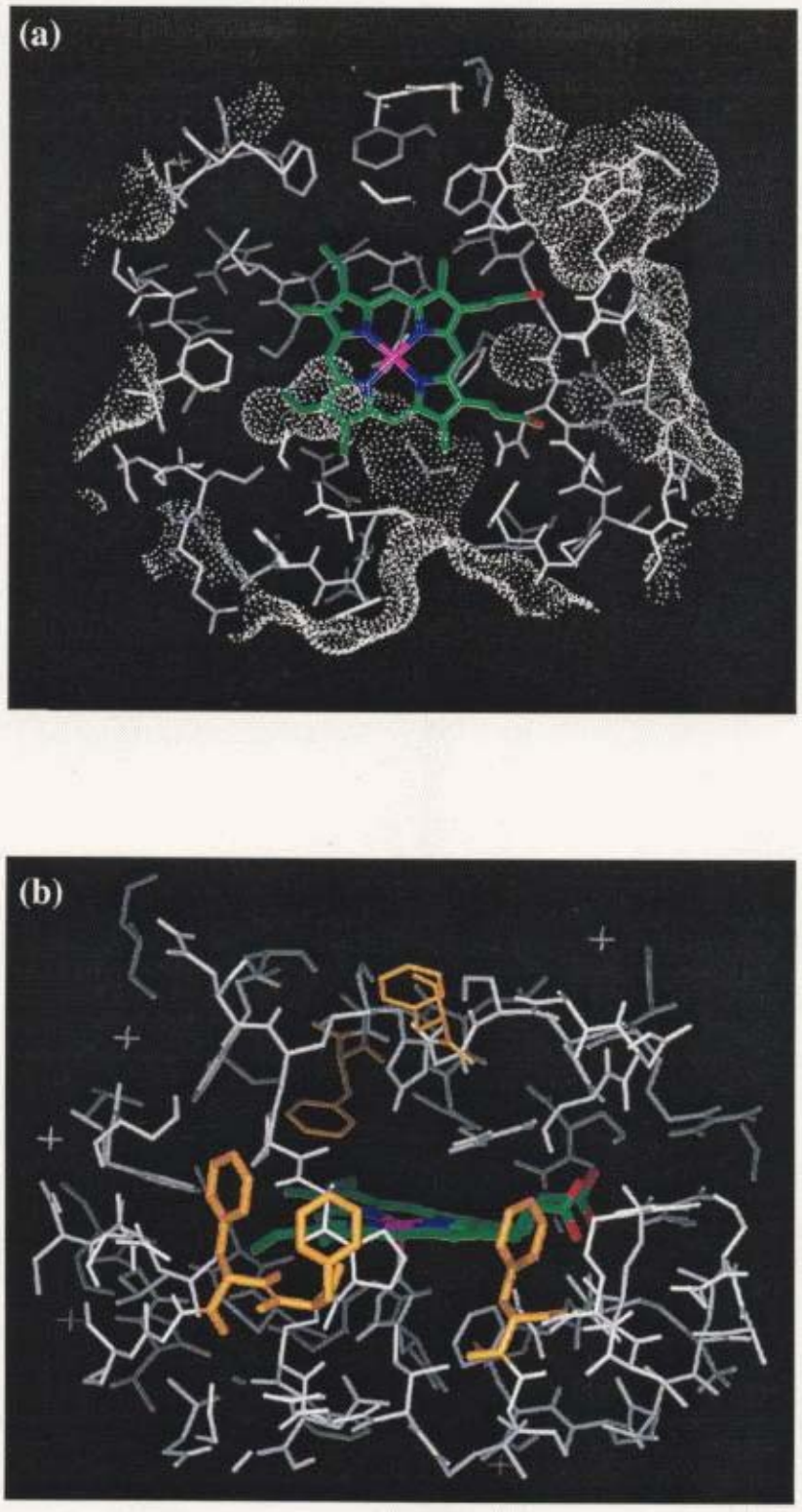

Figure 2.3.6. Substrate access channel of horseradish peroxidase: (a) top view. The solvent accessible surface is drawn by dots; (b) side view. The peripheral phenylalanine residues are highlightened in orange color.

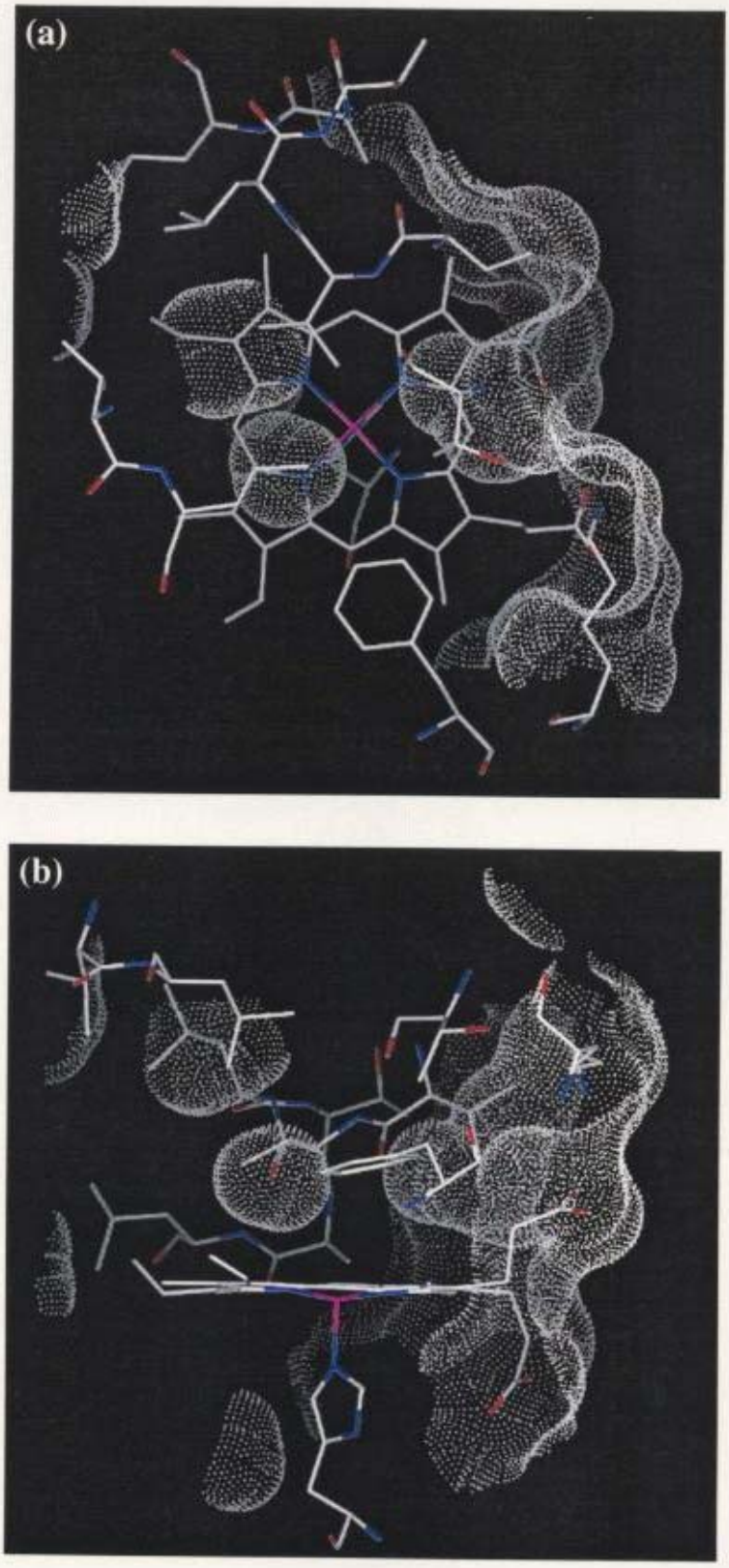

Figure 2.3.7. X-ray crystal structure of heme environment of sperm whale myoglobin His64Thr mutant. (a) top view; (b) side view. The solvent accessible surface is drawn by dots.

a factor of 10 (Table 2.3.2 and Figure 2.3.5). Thus, the active site of H64S Mb is somewhat crowded in comparison with TMPFe complex, and a tiny steric difference of the substrate structure is recognized by the topological factor of H64S Mb mutant (Scheme 2.3.1). Similar steric effects have been observed even in model systems if bulky substituents are introduced into a periphery of the porphyrin ring.[8]

Implication to Cytochrome P450 Reactions. The major biological role of cytochrome P450 is the oxygenation of a variety of substrates. Release of reaction intermediates such as substrate cation radicals and substrate radicals has never observed. For example, hydroxylation of hydrocarbons by compound I of cytochrome P450 has been postulated to involve hydrogen radical abstraction from the substrate to yield an alkyl radical/O=Fe^{IV} pair in the protein active site.[1] The following oxygen rebound to the substrate radical gives the hydroxylation product (Scheme 2.3.3). Very recently, Newcomb et al. have applied hypersensitive radical probe substrates such as (*trans*, *trans*-2-*tert*-butoxy-3-phenylcyclopropyl)methane for understanding of the hydroxylation mechanism.[26] On the basis of the products distribution, the oxygen rebound rates were estimated to be in the range of 10^{10} - 10^{13} s^{-1} if the stepwise hydrogen abstract/oxygen rebound mechanism is correct. In order to introduce the substrate to the active site and to prevent the leakage of substrates (and reaction intermediates) from the active site, P450 provides a substrate access channel and the binding site is in close vicinity of the heme. For example, the X-ray crystal structure of cytochrome $P450_{BM3}$ is depicted in Figure 2.3.8a, which clearly displays the access channel for the substrate from the protein surface to the reaction center which is buried in the protein structure. Figure 2.3.8b also shows the crystal structure of cytochrome $P450_{BM3}$ having the substrate at the heme vicinity.[9] On the basis of these considerations, we believe that the heme environment of H64S Mb is more similar to that of P450 than that of HRP. Direct oxygen transfer into thioanisoles and styrenes by H64S Mb-compound I appears to provide to be good models systems for investigating such reactivity in P450.

Scheme 2.3.3

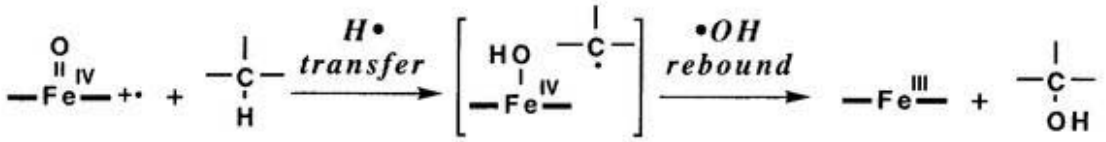

In conclusion, a new protein model system for mechanistic study of cytochrome P450 compound I has been developed, by employment of H64S Mb-compound I. It shows dual modes of reactivity including HRP-like sequential electron transfer and cytochrome P450-like direct oxygen transfer, depending on the redox potential and structure of substrates.

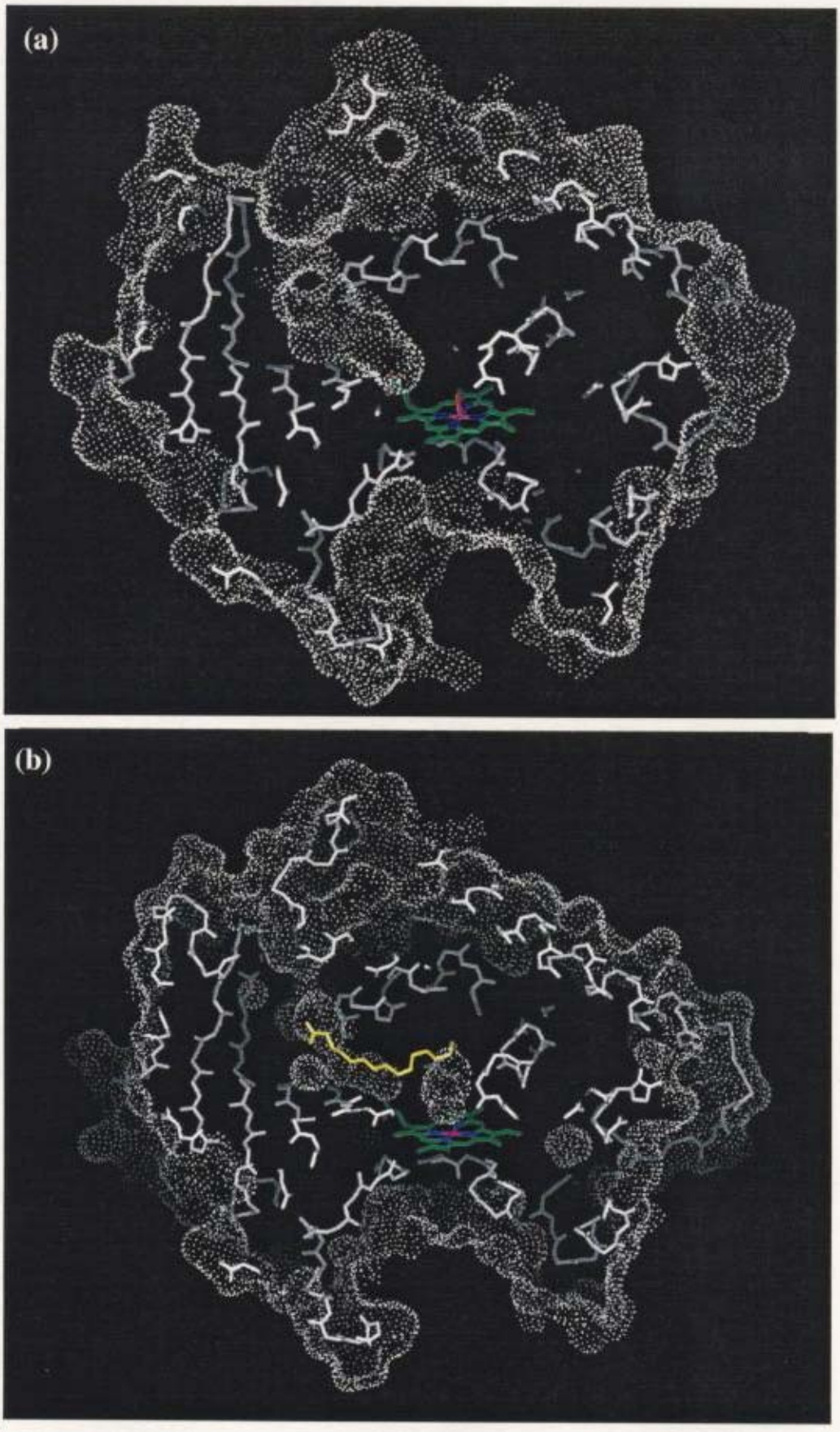

Figure 2.3.8. Sliced view of X-ray crystal structure of $P450_{BM-3}$. (a) substrate-free; (b) complexed with the substrate, palmitoleic acid (yellow). The solvent accessible surface is drawn by dots.

REFERENCE

(1) Ortiz de Montellano, P. R. *Cytochrome P450. Structure, Mechanism, and Biochemistry.;* 2nd ed.; Plenum Publishing Corporation: New York, 1995.

(2) Guengerich, F. P.; Macdonald, T. L. *Acc. Chem. Res.* **1984**, *17*, 9-16.

(3) Egawa, T.; Shimada, H.; Ishimura, Y. *Biochem. Biophys. Res. Commun.* **1994**, *201*, 1464-1469.

(4) Dunford, H. B.; Stillman, J. S. *Cood. Chem. Rev.* **1987**, *19*, 187-251.

(5) Perez, U.; Dunford, H. B. *Biochim. Biophys. Acta.* **1990**, *1038*, 98-104.

(6) Perez, U.; Dunford, H. B. *Biochemistry* **1990**, *29*, 2757-2763.

(7) Matsui, T.; Ozaki, S.; Watanabe, Y. *J. Biol. Chem.* **1997**, *272*, 32735-32738.

(8) Gajhede, M.; Schuller, D. J.; Henriksen, A.; Smith, A. T.; Poulos, T. L. *Nature Struct. Biol.* **1997**, *4*, 1032-1038.

(9) Li, H.; Poulos, T. L. *Nature Struct. Biol.* **1995**, *4*, 140-146.

(10) Quillin, M. L.; Arduini, R. M.; Olson, J. S.; Phillips Jr., G. N. *J. Mol. Biol.* **1993**, *234*, 140-155.

(11) Dinnocenzo, J. P.; Karki, S. B.; Jones, J. P. *J. Am. Chem. Soc.* **1993**, *115*, 7111-7116.

(12) Springer, B. A.; Sliger, S. G. *Proc. Natl. Acad. Sci. USA* **1987**, *84*, 8961-8965.

(13) Goto, Y.; Watanabe, Y.; Fukuzumi, S.; Jones, J. P.; Dinnocenzo, J. P. *J. Am. Chem. Soc.* **1998**, *120*, 10762-10763.

(14) Groves, J. T.; Watanabe, Y. *J. Am. Chem. Soc.* **1986**, *108*, 507-508.

(15) Groves, J. T.; Nemo, T. E. *J. Am. Chem. Soc.* **1983**, *105*, 5786-5791.

(16) Groves, J. T.; Watanabe, Y. *J. Am. Chem. Soc.* **1988**, *110*, 8443-8452.

(17) Kobayashi, S.; Nakano, M.; Kimura, T.; Schaap, A. P. *Biochemistry* **1987**, *26*, 5019-5022.

(18) Doerge, D. R. *Arch. Biochem. Biophys.* **1986**, *244*, 678-85.

(19) Doerge, D. R.; Cooray, N. M.; Brewster, M. E. *Biochemistry* **1991**, *30*, 8960-4.

(20) Kobayashi, S.; Nakano, M.; Goto, T.; Kimura, T.; Schaap, A. P. *Biochem. Biophys. Res. Commun.* **1986**, *135*, 166-171.

(21) Wilson, G. S.; Swanson, D. D.; Klug, J. T.; Glass, R. S.; Ryan, M. D.; Musker, W. K. *J. Am. Chem. Soc.* **1979**, *101*, 1040-1042.

(22) Ortiz de Montellano, P. R. *Acc. Chem. Res.* **1987**, *20*, 289-294.

(23) Ortiz de Montellano, P. R.; Choe, Y. S.; Catalano, C. E. *J. Biol. Chem.* **1987**, *262*, 11641-11646.

(24) Ortiz de Montellano, P. R. *Ann. Rev. Pharmacol. Toxicol.* **1992**, *32*, 89-107.

(25) Ringe, D.; Pesto, G. A.; Kerr, D. E.; Ortiz de Montellano, P. R. *Biochemistry* **1984**, *23*, 2-4.

(26) Toy, P. H.; Newcomb, M.; Hollenberg, P. H. *J. Am. Chem. Soc.* **1998**, *120*, 7719-7729.

PART III

Reactivity of Peroxoiron(III) Porphyrin Complexes: Models for Deformylation Reactions Catalyzed by Cytochrome P450

published in *Journal of Inorganic Biochemistry* **1998,** *69,* 241-247.

Yoshio Goto, Senji Wada, Isao Morishima, and Yoshihito Watanabe

ABSTRACT: Oxoiron(IV) porphyrin π-cation radical is considered as a common reactive intermediate in cytochrome P450 catalyzed monooxygenation. However, a ferric peroxo complex has been also proposed as a reactive intermediate in deformylation reactions catalyzed by cytochrome P450s. In spite of the importance of the peroxo complex in biological functions, reactivities of the peroxo complex have not been well elucidated. Thus, we employed several peroxo-Fe^{III}TPP derivatives to examine the reactions with alkyl aldehydes. A reaction of $[TPPFe(III)O_2]^-K^+$ (TPP = tetrakis-5,10,15,20-phenylporphyrin dianion) with cyclohexanecarboxyaldehyde in acetonitrile under He atmosphere gave cyclohexanone as a deformylated compound, along with 3-cyclohexylacrylonitrile, which was formed by the condensation of the aldehyde with acetonitrile. Similar reactions were also observed when other aldehydes were employed as the substrate. We propose that ferric peroxo porphyrin complex attacks aldehyde carbon as a nucleophile in these reactions. Those aldehydes were simply oxidized to the corresponding carbonic acids when $O=Fe^{IV}$TMP (TMP = tetrakis-5,10,15,20-mesitylporphyrin dianion) π-cation radical was used as the oxidant. The results by these model studies indicate possible intermediacy of the peroxo complex in deformylation reactions observed in P450 systems.

ABBREVIATIONS

TPP	tetrakis-5,10,15,20-phenylporphyrin dianion
TDCPP	tetrakis-5,10,15,20-(2,6-dichrolophenyl)porphyrin dianion
TMP	tetrakis-5,10,15,20-mesitylporphyrin dianion
m-CPBA	3-chloroperbenzoic acid.

INTRODUCTION

Cytochrome P450 is a family of heme containing monooxygenases which reductively activate molecular oxygen to metabolize xenobiotics and steroids by hydroxylation, epoxidation, or *N*- and *O*-dealkylation.[1] In the catalytic cycle of cytochrome P450, an oxoferryl (Fe^{IV}=O) porphyrin π-cation radical (or its equivalent) through the heterolytic O-O cleavage of a ferric peroxo complex (Fe^{III}-O-O^-) has been postulated as the reactive intermediate. Most of the oxidations catalyzed by cytochrome P450 can be explained by assuming the oxoferryl species.[2] In the case of aldehyde oxidation by cytochrome P450, two different types of oxidation have been observed. One is the straightforward oxidation of aldehyde to the carboxylic acid (RCHO → RCO_2H).[2-4] Examples of this type of reactions are cytochrome P450 catalyzed oxidation of acetaldehyde,[5] saturated aliphatic aldehydes,[6,7] α,β–unsaturated aliphatic aldehydes.[6, 8-10]

The second type of the oxidation is rather unusual.[2,11-16] The ferric peroxo intermediate is proposed to attack the aldehyde carbon directly as a nucleophile. A peroxo-substrate adduct finally yields formic acid and deformylated products. Key pieces of evidence supporting this mechanism include the finding that the reaction is supported both by NADPH/O_2 and by H_2O_2 but not by alkylhydroperoxides, peracids, and iodosobenzene.[11] For example, the cytochrome P450 catalyzed decarboxylation of aldehydes was observed in the demethylation reactions by lanosterol 14-demethylase[12] and aromatase.[13]

Placental aromatase is responsible for the transformation of androgens **1** to estrogens **3** at the expense of 3 mol each of NADPH and O_2 according to three stepwise reactions shown in Scheme 1.[13] The reaction is initiated by C-19 hydroxylation of **1** and subsequent oxidation gives a C-19 oxo intermediate **2**. The final step in the aromatase reaction is the oxidative deformylation of **2** yielding **3** and formic acid. If a high valent oxo species is the reactive intermediate in the final step, the products are expected to be

derivatives of the 19-carboxylic acid intermediate.[14,15b] Thus, direct participation of the peroxoiron(III) porphyrin complex for the transformation of **2** to **3** has been proposed.[15-17] Not only the case of lanosterol 14-demethylase and aromatase, the decarboxylation of xenobiotic aldehydes has now been observed in the oxidation of isobutyraldehyde,[18] trimethylacetaldeyde,[18] citronellal,[18] cyclohexanecarboxaldehyde,[11] and 3-oxodecalin-4-ene-10-carboxaldehyde.[19]

Scheme 3.1

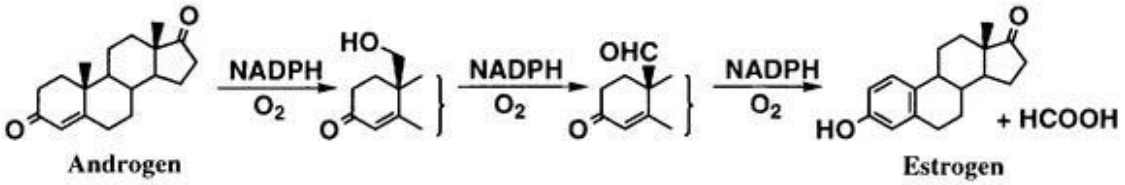

Androgen **Estrogen**

1 **2** **3**

In order to understand more detail about the deformylation by the peroxo-iron(III) intermediate, studies by employing synthetic model systems seem to be very important. Unfortunately, a few works have been reported[20-23] since the first successful preparation of peroxo-Fe(III)TPP and peroxo-Fe(III)OEP by Valentine et al.[24] In this paper, we report the reactions of peroxo-Fe(III)TPP derivatives and a series of aldehydes.

EXPERIMENTAL PROCEDURE

General Procedure. Due to instability of peroxoiron(III) porphyrin complexes upon exposure to moisture, all reactions including preparation of the ferric peroxo complexes were carried out in a glove box filled with dry helium (99.9999%) unless otherwise noted. Acetonitrile was rigorously dried before use: HPLC grade acetonitrile was stirred over KO_2 (Aldrich) in a glove box for 1h and subsequently passed through Super I acidic alumina (ICN).

Instruments. UV-visible spectra were measured on a SHIMADZU UV1200

spectrometer in a glove box filled with dry helium, or on a SHIMADZU UVPC2400 spectrometer with screw-capped cells. Electron paramagnetic resonance (EPR) measurements were carried out at X-band (9.15 GHz) microwave frequency on a Brucker ESP300E Electron Spin Resonance spectrometer with X-band cavity at 4K, or on a JEOL JES-FE2XG Electron Spin Resonance spectrometer with X-band cavity at 77K, by operating with 100-kHz magnetic field modulation. Product analyses were carried out by a SHIMADZU QP-5000 Gas Chromatography Mass Spectrometer (Shimadzu capillary column; HiCap-CBP1, 25m) with electron ionization voltage at 1.5 eV.

Materials. Commercially available reagents from Aldrich, Wako Chemical and Nacalai Tesque were used without further purification unless otherwise noted. Phenyl acetaldehyde and 2-phenylpropionaldehyde were distilled under reduced pressure and stored in a glove box. Tetraphenylporphyrin [$TPPH_2$], tetramesitylporphyrin [$TMPH_2$], and tetrakis(2,6-dichlorophenyl)porphyrin [$TDCPPH_2$] were prepared by modification of methods reported.[25] Iron was inserted to the porphyrins to form ferric porphyrin chloride complexes by a standard method.[26]

Preparation and Reactions of Peroxo Complexes under He Atmosphere. $K^+[PorFe(III)O_2]^-$ was prepared *in situ* by stirring PorFe(III)Cl (3.75 mM) with two equivalent of 18-crown-6 ether and a large excess of KO_2 powder in dry acetonitrile for 15 min followed by filtration to remove unreacted KO_2.[23,24] After confirmation of the peroxo complex formation by UV-visible measurement, a dry acetonitrile solution of a substrate was added to the $K^+[PorFe(III)O_2]^-$ solution (0.5 mL, 3.75 mM) under He atmosphere at room temperature (final concentration, 2.5 mM for $K^+[PorFe(III)O_2]^-$ and 5 mM for the substrate). The reaction mixture was stirred for 1 hr under He atmosphere and the products were analyzed by GC-MS.

Reaction of Fe(IV)=O Porphyrin π−cation Radical with Aldehyde. To a methylene chloride solution of $TMPFe^{III}Cl$ (1.0mM) was added 4 equivalent of mCPBA

at -80°C and the reaction mixture was stirred. After confirmation of TMPFe(IV)=O π-cation radical formation[27] by the solution color change to green, 2 equivalent of cyclohexanecarboxyaldehyde was added and stirred for 30 min. The reaction mixture was then treated with diazomethane and submitted to GC-MS to identify cyclohexanecarboxylic acid as a methyl ester.

Preparation of Substrates and Authentic Samples of Oxidation Products

2-Cyclohexylacrylonitrile (6). To a THF (35mL) suspension of sodium hydride (585mg, 14.6 mmol; commercial 60% oil dispersion) was added dropwise a solution of diethyl cyanomethylphosphonate (2.14 mL, 14.1 mmol) in THF (17.5 mL) at 0°C and stirred for 15 min. Then the solution was warmed to r.t. and a THF (17.5 mL) solution of cyclohexanecarboxyaldehyde (1.26 mL, 10.5 mmol) was added dropwise and stirred at r.t. for 3hr. The reaction mixture was washed with water. The organic layer was extracted with dichloromethane and the solvent was evaporated. The remaining liquid was purified by distillation to give colorless oil (50 % yield). ^{1}HNMR ($CDCl_3$):δ 1.05-1.80 (m, 10H), 2.5-2.75 (m, 1H), 5.20 (d, J = 11 Hz, 1H), 6.31 (t, J = 10Hz, 1H).

2-Methyl-2-phenylpropionaldehyde (10). To a THF (50mL) suspension of sodium hydride (880mg, 22 mmol; commercial 60% oil dispersion) was added dropwise 2-phenylpropionaldehyde (2.65 mL, 20 mmol) in THF (10 mL) at 0°C. After stirring for 5 min, iodomethane (1.37 mL, 22 mmol) in THF (10 mL) was added dropwise and stirred at room temperature for 10hr. The reaction mixture was washed with water, then organic layer was extracted with diethylether and the solvent was evaporated. The remaining liquid was purified by distillation under reduced pressure (20 mmHg, 82-85°C) to give colorless oil (50 % yield). ^{1}HNMR ($CDCl_3$):δ 1.47 (s, 6H), 7.20-7.40 (m, 5H), 9.51 (s, 1H).

2-(Benzyldimethyl)methylacrylonitrile. To a THF (17mL) suspension of sodium hydride (240mg, 6.0 mmol; commercial 60% oil dispersion) was added dropwise diethyl cyanomethylphosphonate (0.88 mL, 5.8 mmol) in THF (8.5 mL) at 0°C and

stirred for 10 min. Then 2,2-dimethyl-3-phenylpropionaldehyde (754 mg, 4.65 mmol) in THF (8.5 mL) was added dropwise and stirred at room temperature for 20hr. The reaction mixture was washed with water and the organic layer was extracted with dichloromethane, followed by evaporation of the solvent. The residue was submitted to a column chromatograph (silica gel, hexane : ethyl acetate = 5 : 1) to give a *cis*- and *trans*-isomer as colorless liquid (50 % yield).^{1}HNMR ($CDCl_3$):δ for *trans*-isomer, 1.06 (s, 6H), 2.64 (s, 2H), 5.10 (d, J = 16 Hz, 1H), 6.74 (d, J = 16Hz, 1H), 7.05-7.30 (m, 5H), for *cis*-isomer, 1.28 (s, 6H), 2.75 (s, 2H), 5.28 (d, J = 12 Hz, 1H), 6.32 (d, J = 12Hz, 1H), 7.05-7.30 (m, 5H).

2,2-Dimethyl-3-phenylpropionaldehyde (11). To a suspension of pyridinium chlorochromate (6.47 g, 30 mmol) in dry dichloromethane (40 mL) was added 2,2-dimethyl-3-phenylbutanol (3.29 g, 20 mmol) in dry dichloromethane (4 mL) in one portion with vigorous stirring. After stirring at room temperature for 90 min, 100 mL of diethylether was added and the resulting solution was passed through a silica gel column for removal of solid residues. The solvent was evaporated and then the remaining oil was purified by distillation under reduced pressure (20 mmHg, 103-106°C) to give colorless liquid (56 % yield). ^{1}HNMR ($CDCl_3$):δ 1.05 (s, 6H), 2.78 (s, 2H), 7.07-7.30 (m, 5H).

2-(Dimethylphenyl)methylacrylonitril (2-cumylacrylonitril). To a THF (10mL) suspension of sodium hydride (240mg, 6.0 mmol; commercial 60% oil dispersion) was added dropwise diethyl cyanomethylphosphonate (0.88 mL, 5.8 mmol) in THF (8.5 mL) at 0°C and stirred for 10 min. Then 2,2-dimethyl-3-phenylpropionaldehyde (740 mg, 5.0 mmol) in THF (8.5 mL) was added dropwise and stirred at room temperature for 20hr. The reaction mixture was washed with water and the organic layer was extracted with dichloromethane, followed by evaporation of the solvent. The residue was submitted to a column chromatograph (silica gel, hexane : ethyl acetate = 5 : 1) to give colorless liquid as a mixture of *cis*- and *trans*- isomer (48 %

yield).^{1}HNMR ($CDCl_3$):δ for *cis*-isomer, 1.64 (s, 6H), 5.36 (d, J = 12 Hz, 2H), 6.53 (d, J = 12Hz, 1H), 7.24-7.38 (m, 5H), for *trans*-isomer, 1.45 (s, 6H), 5.28 (d, J = 17 Hz, 1H), 6.32 (d, J = 17 Hz, 1H), 7.24-7.38 (m, 5H).

3.3 RESULTS AND DISCUSSION

Peroxoiron(III) species in the catalytic cycle of cytochrome P450 has been postulated as a key intermediate to afford a high valent species equivalent to compound I of peroxidases. In 1980, Valentine et al. reported the preparation of peroxo-Fe^{III}(TPP) and peroxo-Fe^{III}(OEP) by the reactions of KO_2 with Fe^{III}(TPP)Cl and Fe^{III}(OEP)Cl in aprotic solvents.[24] Examination of the complexes by NMR, ESR, UV, IR, and EXAFS supports the structure of the complexes to be ferric-peroxo species with side-on structure as shown below.[24] The same peroxo complexes could be obtained either by the reaction of Fe(I) porphyrin with O_2 or by the reduction of oxy complexes.[28] The latter reaction is the exact model reaction of the cytochrome P450 catalyzed oxygen activation. Similar reactions were also applied for the preparation of peroxo-Mn porphyrin complexes.[29] The X-ray structure of peroxo-Mn^{III}(TPP) revealed an unusually domed structure of the complex.[30] Reactions of this type of peroxo complexes might be good models for the peroxo intermediate in cytochrome P450.

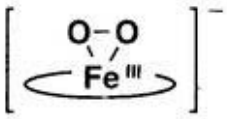

Reaction of Alkyl Aldehydes with Peroxoiron(III) Porphyrin Complexes. A reaction of [$TPPFe^{III}(O_2)$]$^-$ and cyclohexanecarboxyaldehyde **4** took place in acetonitrile at room temperature under dry helium atmosphere. According to the reaction, the UV-vis spectral change of [$TPPFe^{III}(O_2)$]$^-$ was observed (Figure 3. 1). The oxidation products of **4** were determined by GC-MS. Cyclohexanone **5** was identified (yield, 15 %) as the deformylated product along with *cis*- and *trans*-isomers of 3-

cyclohexyl-acrylonitrile **6** (total yield, 20 %) (run 1 in Table 3.1, eq (1)), which are formed by condensation of **4** and acetonitrile. Similar reactions of **4** with a series of peroxoiron(III) porphyrin complexes were also carried out and the results are summarized in Table 3.1. While the deformylated product **5** was obtained in the reaction of **4** with $[Fe^{III}TDCPP(O_2)]^-$ under He atmosphere, $[Fe^{III}TMP(O_2)]^-$ gave a trace amount of **5**. As shown in Table 3.1, the reaction of KO_2 and **4** also gave **6**, thus, possible participation of free KO_2 even in the peroxo-Fe complex reactions was examined. However, ESR examination of the solution clearly showed no contamination of superoxide anion in the solution (Figure 3. 2).

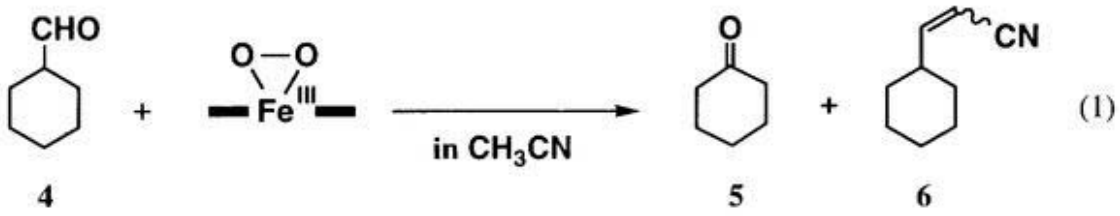

4 5 6 (1)

Table 3.1. Reaction of Cyclohexanecarboxyaldehyde (4) with Peroxoiron(III) Porphyrin Complexes

run	condition	percent yields of products [%] [a]	
		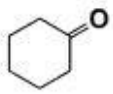	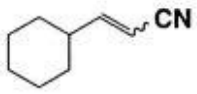
		5	**6**
1	$[Fe^{III}TPP(O_2)]^-$	15	20
2	$[Fe^{III}TPP(O_2)]^-$ / PBN [b]	8	15
3	$[Fe^{III}TMP(O_2)]^-$	trace	50
4	$[Fe^{III}TDCPP(O_2)]^-$	18	5
5	KO_2	trace	40

[a] Yields were determined by GC-MS based on peroxoiron(III) porphyrin complex used. [b] [PBN] = 10 mM.

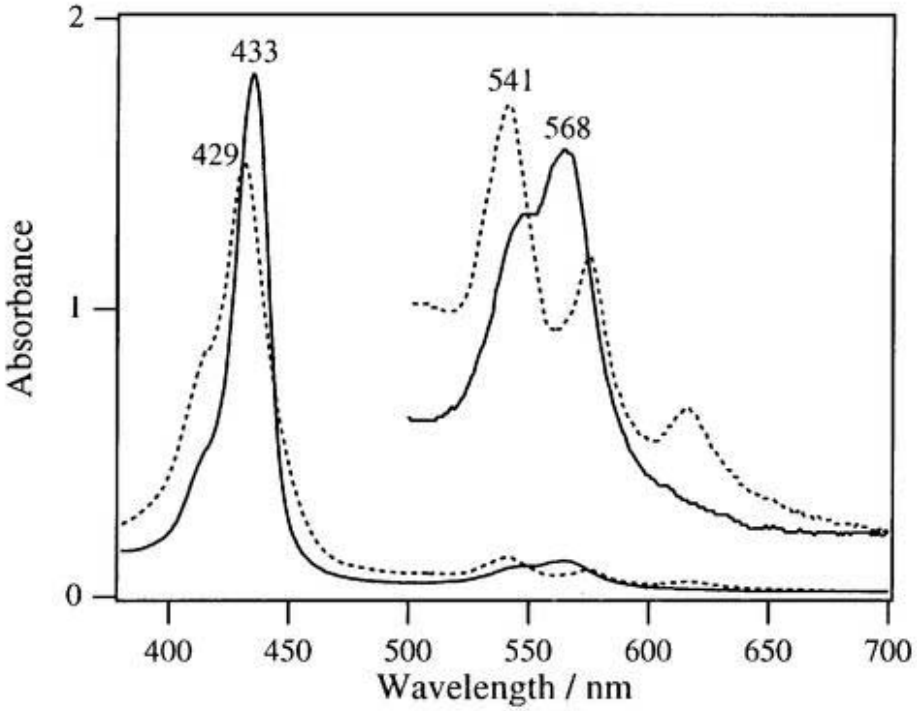

Figure 3.1. UV-vis spectral change in the reaction of $[Fe^{III}TPP(O_2)]^-$ upon the addition of **4** at room temprature.

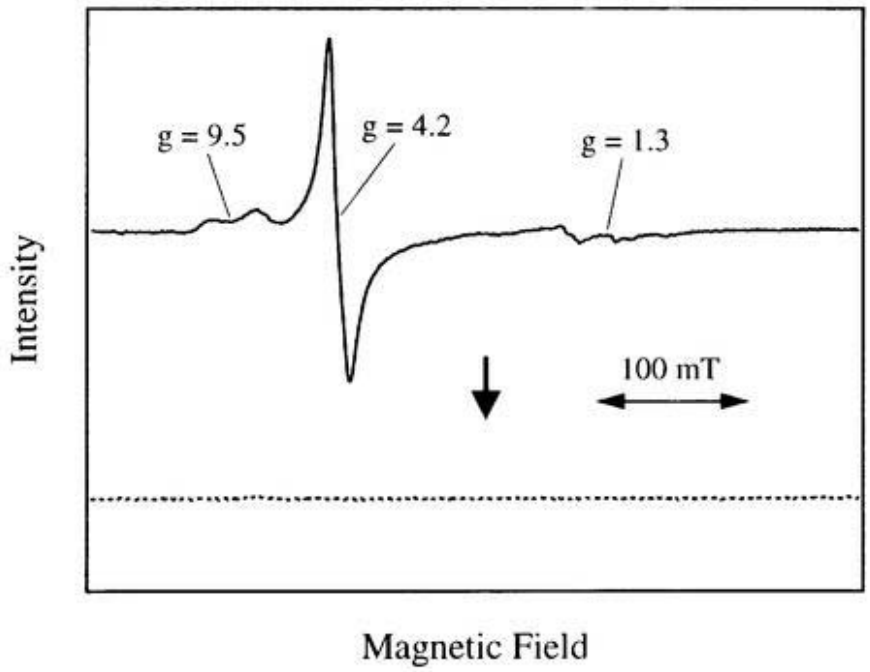

Figure 3.2. ESR spectra (at 4K) before (solid) and after (dotted) the addition of **4** to CH_3CN solution of $[Fe^{III}TPP(O_2)]^-$ at room temperature.

Deformylation in the same manner was also observed in the reactions of peroxo-iron(III) complexes with phenylacetaldehyde (**7**) and 2-phenylpropionaldehyde (**8**). The reactions of **7** and peroxo-iron(III) complexes gave a trace amount of benzaldehyde, while 15 ~ 30 % yields of acetophenone (**9**) were observed for the oxidation of **8**. Incidentally, the reactions of **8** with KO_2 gave **9** in yield of 25 %. In reactions of $[TPPFe^{III}(O_2)]^-$ and aldehydes bound to the tertiary carbon such as 2-methyl-3-phenylpropionaldehyde (**10**) or 2,2-dimethyl-3-phenylpropionaldehyde (**11**), the corresponding condensation products with acetonitrile were obtained without deformylated compound (Table 3.2). This indicates α–hydrogen is crucial for the deformylation reaction. Apparently, the yields of deformation reactions are very much dependent on the structure of both substrate and porphyrin.

The results summarized in Tables 1 and 2 indicate that the peroxo complexes serve as a base as well as the deformylating reagent. Though the peroxo-Fe complexes readily react with proton derived from a trace amount of such as methanol and H_2O to afford hydroxo-Fe(III) porphyrins, the peroxo complexes are stable in dry acetonitrile, indicating the peroxo-oxygen is not able to abstract a proton from acetonitrile. Thus, the reaction of the peroxo complex with aldehyde must afford very basic intermediate. Scheme 2 shows a plausible mechanism for the formation of condensation products. The

Scheme 3.2

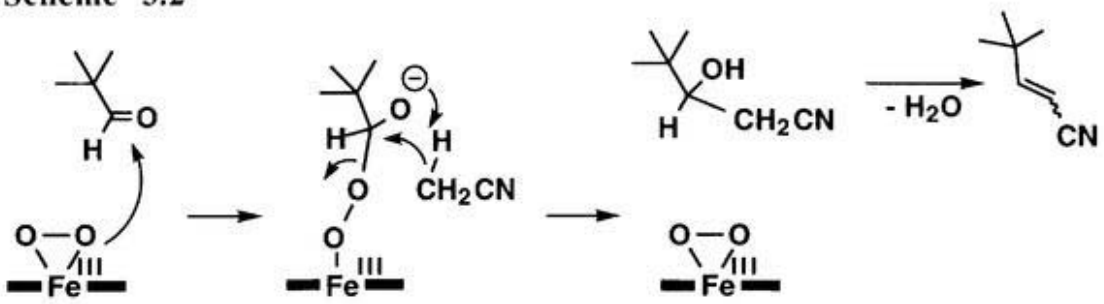

[A]

Table 3.2. Reaction of Aldehydes with Peroxoiron(III) Porphyrin Complexes

Substrate	Complex	Product yield [%] [a]	
		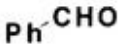	
 **7**	TPP	trace	trace
	TMP	trace	trace
	TDCPP	2	trace
	KO_2	trace	trace
		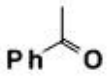	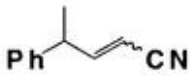
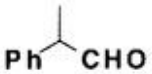 **8**	TPP	15	trace
	TMP	30	trace
	TDCPP	15	trace
	KO_2	25	trace
			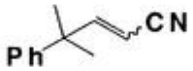
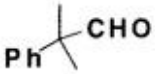 **10**	TPP		30
	TMP		40
	TDCPP		40
	KO_2		58
			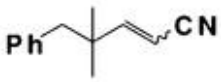
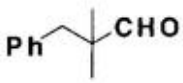 **11**	TPP		13
	TMP		15
	TDCPP		trace
	KO_2		trace

[a] Yields were determined by GC-MS based on peroxoiron(III) porphyrin complex used.

initial nucleophilic attack of the peroxo complex to aldehyde is consistent with its reaction with acyl halides,[21] sulfur dioxide,[22] and carbon dioxide.[23] The peroxo complexes were also prepared in THF to avoid the involvement of the solvent into the products. Unfortunately, the peroxo complexes did not react with aldehydes in THF at room temperature.

In order to gain mechanistic details of deformylation reactions, ESR and UV-vis spectral changes upon addition of aldehydes to the peroxo complexes were measured (Figure 3. 1 and 3. 2). To an acetonitrile solution of $[Fe^{III}TPP(O_2)]^-$ (2.5 mM) two equivalents of **4** was added and stirred for 30 min. Then, the ESR spectrum of the reaction mixture was examined. A typical rhombic ESR signal for the peroxo complexes (g=9.5, 4.2, 1.3) disappeared, and the solution became EPR silent.[25] This spectral change corresponds to the Soret band shift from 432 nm to 429 nm shown in Figure 3. 1. These results suggest that $[Fe^{III}TPP(O_2)]^-$ was changed to Fe(II)TPP according to the reaction with aldehydes.

One of possible mechanisms for the formation of Fe(II)TPP is a homolytic cleavage of Fe-O bond of the ferric peroxy hemiacetal anionic intermediate [A] as shown in Scheme 3. The resulting alkyl peroxy hemiacetal anion radical species could also be an intermediate formed by the direct reaction of **4** and superoxide anion. If this is the case, the deformylation and condensation with solvent share the same intermediate [A] and the following competitive Fe-O cleavage (Scheme 3) and deprotonation (Scheme 2) afford a mixture of products. In order to detect radical species present in the solution, radical trap experiments were carried out. However, the reactions of **4** and $[Fe^{III}TPP(O_2)]^-$ in the presence of phenyl-*tert*-butylnitrone (PBN) as a radical trap reagent under He atmosphere (Table 3.1, run 2) afforded **5** without appreciable effect. This result implies no stable radical species in the solution. In addition, UV-vis spectral changes according the reaction of $[TPPFe^{III}(O_2)]^-$ and aldehyde is very different from that obtained by the reaction of $[TPPFe^{III}(O_2)]^-$ and proton derived from such as methanol, benzoic acid, or

Scheme 3.3

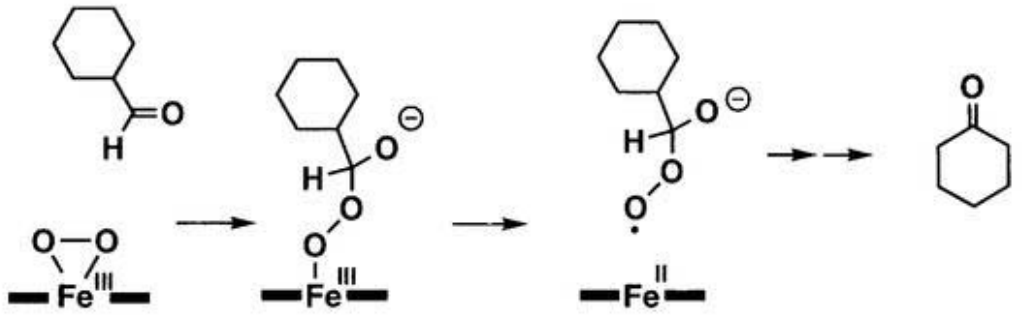

[A]

H_2O. Therefore, direct proton abstract from the substrate by the peroxo complex is a quite unlikely process.

While we could not observe formic acid to be formed along with deformylated ketones, we have obtained a comparable amount of a formic acid equivalent, benzoic acid, to propiophenone when we used 2-phenylbutyrophenone as the substrate (Scheme 3.4).

Scheme 3.4

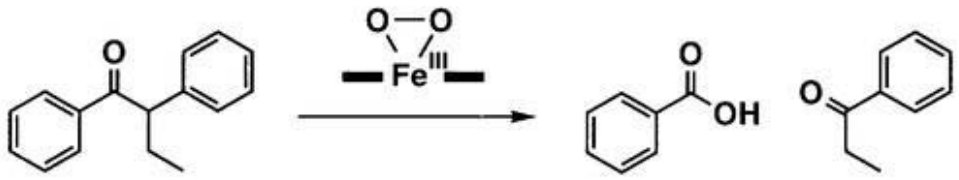

Reaction of Fe(IV)=O Porphyrin π-cation Radial with Alkyl Aldehydes. It has been reported that aldehydes were readily oxidized to carboxylic acids by an oxoferryl porphyrin π-cation radical species,[15] a model complex for the active species responsible for oxidations by peroxidase and cytochrome P450. Indeed, the reaction of **4** and O=Fe(IV)TMP π-cation radical at -80°C generated cyclohexane carboxylic acid in a quantitative yield. Thus, high valent oxo-species are not responsible for the

deformylation. Our results are rather suggestive of the peroxo-Fe^{III} complexes being the active species for the deformylation process. However, there is the crucial difference in the deformylation reactions catalyzed by P450 and our system; i.e., the model system failed to yield olefins. Not only the deformylation, oxidation of hydrocarbons catalyzed by iron porphyrin complexes use to give alcohols and ketones but not olefins even though dehydration (olefin formation) can be observed in heme enzymes catalyzed oxidations.

Very recently, Valentine and coworkers reported epoxidation of α,β-unsaturated ketone by peroxo-Fe^{III}TMP.[20] The reaction could be explained by the initial nucleophilic Michael addition of the peroxo oxygen as observed in the epoxidation of α,β-unsaturated ketone by H_2O_2 under basic condition.[31] These results suggest that the peroxo-Fe^{III} intermediate in the catalytic cycle of P450 could be either trapped by those electrophilic substrates or further activated to high valent oxo-species by its reaction with proton.

In summary, we have examined the reactions of peroxo-Fe^{III} porphyrin complexes with a series of aldehydes. While condensation of aldehydes with solvent acetonitrile masked the oxidation process, we have shown that the deformylation can be conducted only by the peroxo species but not by an oxo-ferryl porphyrin π-cation radical.

REFERENCE

(1) Watanabe, Y. In *Oxygenase and Model Systems,* Funabiki, T., Ed., Kluwer Academic Publishers, The Netherlands, 1997, pp. 223-232.

(2) Ortiz de Montellano, P. R. In *Cytochrome P450. Structure, Mechanism, and Biochemistry,* Ortiz de Montellano, P. R., Ed., Plenum Publishing Corporation, New York, 1995, 2nd ed., pp 245-303.

(3) Yamamoto, I.; Watanabe, K.; Narimatsu, S.; Yoshimura, H. *Biochem. Biophys. Res. Commun.*, **1988,** *153,* 779.

(4) Watanabe, Y.; Narimatsu, S.; Yamamoto, I.; Yoshimura, H. *J. Biol. Chem.*, **1991,** *266,* 2709.

(5) Terelius, Y.; Norsten-Hoog, C.; Cronholm, T.; Ingelman-Sundberg, M.; *Biochem. Biophys. Res. Commun.*, **1991,** *179,* 689.

(6) Watanabe, K.; Matsunaga, T.; Narimatsu, S.; Yamamoto, I.; Yoshimura, H. *Biochem. Biophys. Res. Commun.*, **1992,** *188,* 114.

(7) Davis, S. C.; Sui, Z.; Peterson, J. A.; Ortiz de Montellano, P. R. *Arch. Biochem. Biophys.*, **1996,***328,* 35.

(8) (a) Watanabe, K.; Matsunaga, T.; Yamamoto, I.; Yoshimura, H. *Drug. Metab. Dispos.*, **1995,** *23,* 261. (b) Watanabe, K.; Narimatsu, S.; Matsunaga, T.; Yamamoto, I.; Yoshimura, H. *Biochem. Pharmacol.*, **1993,** *46,* 405.

(9) Tomita, S.; Tsujita, M.; Matsuo, Y.; Yubisui, T.; Ichikawa, Y. *Int. J. Biochem.*, **1993,** *25,* 1775.

(10) Stearns, R. A.; Chakravarty, P. K.; Chen, R.; Chiu, S.-H. L. *Drug. Metab. Dispos.*, **1995,** *23,* 207.

(11) Vaz, A. D. N.; Roberts, E. S.; Coon, M. J. *J. Am. Chem. Soc.*, **1991,** *113,* 5886,

(12) Fischer, R. T.; Trzaskos, J. M.; Magolda, R. L.; Ko, S. S.; Brosz, C. S.; Larsen, B. *J. Biol. Chem.*, **1991,** *266,* 6124. references therein.

(13) (a) Thompson, E. A.; Siiteri, P. K. *J. Biol. Chem.*, **1974,** *249,* 5373. (b) Thompson, E. A.; Siiteri, P. K. *J. Biol. Chem.*, **1974,** *249,* 5364. (c) Meyer, A. S. *Biochem. Biophys. Acta*, **1955,** *17,* 441. (d) Arigoni, D.; Bataglia, R.; Akhtar, M.; Smith, T. J. *J. Chem. Soc., Chem. Commun.*, **1975,** 185.

(14) Watanabe, Y.; Takehira, K.; Shimizu, M.; Hayakawa, T.; Orita, H. *J. Chem. Soc., Chem. Commun.*, **1990,** 927.

(15) (a) Watanabe, Y.; Ishimura, Y. *J. Am. Chem. Soc.*, **1989,** *111,* 8047. (b) Watanabe, Y.; Ishimura, Y. *J. Am. Chem. Soc.*, **1989,***111,* 410.

(16) Cole, P. A.; Robinson, C. H. *Proc. Natl. Acad. Sci.*, **1990,** *87,* 2999.

(17) (a) Stevenson, D. E.;Wright, J. N.; Akhtar, M. *J. Chem. Soc., Perkin Trans. I*, **1988,** 2043. (b) Akhtar, M.; Calder, M. R.; Corina, D. L.; Wright, J. N. *Biochem. J.*, **1982,** *201,* 569.

(18) Roberts, E. S.; Vaz, A. D. N.; Coon, M. J. *Proc. Natl. Acad. Sci. USA,* **1991,** *88,* 8963.

(19) Vaz, A. D. N.; Kessell, K. J.; Coon, M. J. *Biochemistry*, **1994,** *33,* 13651.

(20) (a) Selke, M.; Sisemore, M. F.; Valentine, J. S. *J. Am. Chem. Soc.*, **1996,** *118,* 2008. (b) Sisemore, M. F.; Burstyn, J. N.; Valentine, J. S. *Angew. Chem. Int. Ed. Engl.*, **199635,** 206. (c) Sisemore, M. F.; . Selke, M.; Burstyn, J. N.; Valentine, J. S. *Inorg. Chem.*, **1997,** *36,* 979. (d) Selke, M.; Sisemore, M. F.; Ho, R. Y. N.; Wertz, D. L.; Valentine, J. S. *J. Mol. Catal. A,* **1997,** *117,* 71.

(21) Khenkin, A. M.; Shteinman, A. A. *J. Chem. Soc., Chem. Commun.*, **1984,** 1219.

(22) Miksztal, A. R.; Valentine, J. S. *Inorg. Chem.*, **1984,** *23,* 3548.

(23) Schappacher, M.; Weiss, R.; Montiel-Montoya, R.; Trautwein, A.; Tabard, A. *J. Am. Chem. Soc.*, **1985,** *107,* 3736.

(24) (a) Bustyn, J. N.; Roe, J. A.; Miksztal, A. R.; Shaevitz, B. A.; Lang, G.; Valentine, J. S. *J. Am. Chem. Soc.*, **1988,** *110,* 1382. (b) McCadish, E.;

Miksztal, M. N. A. R.; Sprenger, A. Q.; Valentine, J. S.; Strong, J. D.; Spiro, T. G. *J. Am. Chem. Soc.*, **1980,** *102,* 4268.

(25) Lindsey, L. S.; Wagner, R. W. *J. Org. Chem.*, **1989,***54,* 828-836.

(26) Kobayashi, H.; Higuchi, T.; Kaizu, Y.; Osada, H.; Aoki, M. *Bull. Chem. Soc. Jpn.*, **1975,** *48,* 3137-3141.

(27) (a) Groves, J. T.; Watanabe, Y. *J. Am. Chem. Soc.*, **1986,** *108,* 7834. (b) Groves, J. T.; Watanabe, Y. *J. Am. Chem. Soc.*, **1988,** *110,* 8443.

(28) Welborn, C. H.; Dolphin, D.; James, B. R. *J. Am. Chem. Soc.*, **1981,** *103,* 2869.

(29) Valentine, J. S.; Quinn, A. E. *Inorg. Chem.*, **1976,** *15,* 1997.

(30) VanAtta, R. B.; Strouse, C. E.; Hanson, L. K. *J. Am. Chem. Soc.*, **1987,** *109,* 1425.

(31) (a) Felix, D.; Wintner, C.; Eschenmoser, A. In *Org. Synth. Collective* IV, pp 679-682. (b) L. F. Fieser M. Fieser In *Reagents for Organic Synthesis,* Wiley, New York, 1967, Vol. 1, pp. 466.

PART IV

SUMMARY AND CONCLUSIONS

In most of oxygenation reactions catalyzed by cytochrome P450, a high valent oxo-iron species, $O=Fe^{IV}$ porphyrin π-cation radical, has been attributed to the active species. In fact, similar $O=Fe^{IV}$ porphyrin π-cation radicals, so called compound I, have been characterized as the active intermediates in peroxidases and catalase catalyzed reactions, even though any reactive intermediates equivalent to compound I have never characterized for cytochrome P450. In addition, a peroxo-ferric intermediate of cytochrome P450 has been also considered as an intermediate responsible for a few reactions. Throughout this thesis, the author has been trying to elucidate the reactivities of active intermediates proposed in cytochromes P450 catalyzed reactions to understand how or why cytochromes P450 utilize those active intermediate for the oxidative metabolism of foreign compounds.

In Part II, the author has focuses on the reactivities of compound I intermediate. For this purpose, three different types of compound I have been employed to mimic typical cytochromes P450 catalyzed oxygenations, i.e., compound I of horseradish peroxidase (HRP) and sperm whale myoglobin His64Ser mutant and a synthetic model, $O=Fe^{IV}TMP^{+\bullet}$ (TMP = tetrakis-5,10,15,20-mesitylporphine dianion), since these protein compounds I and their synthetic model are stable enough for the direct measurement of their reactions with substrates such as tertiary amines, sulfides, and olefins by a UV-vis spectroscopy.

In chapter 1, the reaction mechanisms of N-demethylation of N,N-dimethylaniline (DMA) by compounds I have been investigated. The UV-vis spectral change in the reaction of HRP-compound I with DMA showed rapid formation of compound II followed by decay to the ferric resting state. The observation of a sequential electron transfer is consistent with the linear correlation and steepness between logarithm of rate constants for the oxidation of a series of *p*-substituted DMAs by compounds I and one-electron oxidation potential of DMAs. The sequential electron transfer mechanism was further supported by no kinetic isotope effects on the electron transfer processes of deuterated DMA, $PhN(CD_3)_2$, even though product deuterium kinetic isotope effect was observed. On the other hand, the reaction of DMAs by the synthetic model system

showed a 2-electron oxidation process in the UV-vis spectral change, however, the redox dependency of the rate constants in reactions of a series of DMAs is similar to that for HRP system. Together with the isotope effect obtained both in kinetic experiments and product analyses, the reaction mechanism of compound I of TMPFe with DMAs is confirmed to proceed via electron transfer/hydrogen atom transfer.

Chapter 2 deals with the reaction mechanisms of sulfoxidation of thioanisoles and a cyclic sulfide by compounds I. HRP-compound I reacts with thioanisoles to afford HRP-compound II along with the ferric resting state. The rates of oxidations determined by the direct observation of time dependent spectral changes were plotted on to the redox potentials of thioanisoles, and a comparison with that of DMA oxidation by HRP indicates the reactions proceed via electron transfer from thioanisoles to compound I. The redox potential dependency of the sulfoxidation rates by the synthetic model compound I and the Mb mutant compound I are very different from those observed for DMA N-demethylations. At the same time, the rates for the sulfoxidation are much higher than the rates expected for the mechanism which involves one electron transfer from a sulfide to compound I. Thus, those reactions are concluded to proceed via direct oxygen transfer mechanism.

Chapter 3 describes structure-function relationship of the oxidations by H64S Mb mutant compound I. The Mb mutant oxidizes DMA by sequential electron transfer to carry out the N-demethylation whereas the Mb mutant proceeds the sulfoxidation of thioanisoles and the epoxidation of styrenes through two electron oxidation coupled with oxygen transfer into the substrates. 3-D structures of HRP and a H64T Mb mutant indicate that there are huge differences in the three-dimensional structures around the heme vicinity of two enzymes. It seems very hard for substrates to access to the oxygen bound to the heme iron of HRP compound I while H64T Mb mutant provides an access channel for substrates. Thus, HRP compound I mostly oxidizes substrates through electron transfer. On the other hand, the mechanistic features of substrate oxidations by H64S Mb compound I are quite similar to those of the model system. These

considerations are also applied for the cytochrome P450 catalyzed oxygenation mechanisms.

Part III is devoted to understand the reactivity of peroxoferric porphyrin complexes with aldehyde. Cytochromes P450 aromatase and lanosterol 14α-demethylase have been believed to utilize this peroxoferric intermediate for the deformylation of aldehyde groups on a cascade of the steroid biosynthesis. The peroxo intermediate has never been observed in the enzymatic reaction cycle, thus model complexes have been employed. As models TMP, TPP and TDCPP iron complexes have been used. Reactions of peroxo complexes with various kinds of aldehyde give deformylated products, but no example similar to the type of aromatase reaction was obtained. Reaction mechanisms are still not clarified yet, although the results suggest the reactions could involve a base-catalyzed process.

Through those studies, the author has developed a new approach for the elucidation of reaction mechanisms catalyzed by cytochrome P450. The use of Mb mutant compound I as a protein model for cytochrome P450 as well as HRP compound I and synthetic models has allowed us to examine detailed oxidation mechanisms of N-demethylation and sulfoxidation. At the same time, direct observation of these reactions by stopped flow techniques even at very low temperature has provided direct evidence for electron transfer/oxygen transfer mechanisms.

ACKNOWLEDGMENT

The present thesis is a summary of the author's studies from 1996 to 1999 at Department of Structural Molecular Science, the Graduate University for Advanced Studies. This work is generously supported by Institute for Molecular Science and carried out under the supervision of Professor Yoshihito Watanabe. The author wishes to express his cordial gratitude to Professor Yoshihito Watanabe for his continual direction, stimulating discussion, and hearty encouragement. The author also owes his accomplishment of the studies to the discerning advises and helpful discussions by Professor Shunichi Fukuzumi in Osaka University, Shin-ichi Ozaki, Senji Wada, and Toshitaka Matsui in Professor Watanabe's laboratory.

The author is really grateful to Professor Joseph P. Dinnocenzo and Jeffrey P. Jones in University of Rochester for helpful discussions about the study in Chapter 1, Part II.

This work would not have been possible without help of the members and co-workers in the Professor Watanabe's laboratory. The author is deeply indebted to Drs. Seiji Ogo, Mark P. Roach (thanks Mark for proofread and correction of so many manuscripts!), Messrs. Msakazu Iwase, Akira Wada, Shigeyuki Nakamura, Isao Hara, Nobuyuki Makihara, Ryo Yamahara, Miss. Kanazawa, and Mrs. Hui-Jung Yang for valuable suggestions and unfailing encouragement. Acknowledgments are also due to Mrs. Misako Tanizawa and Akiyo Ota for their office works and heartfelt kindness.

Finally, the author expresses his sincere gratitude to his family for their supports, generous understanding, and affectionate encouragement.

Okazaki, January 1999

Yoshio Goto

LIST OF PUBLICATIONS

1 Reactivity of Peroxoiron(III) Porphyrin Complexes: Models for Deformylation Reactions Catalyzed by Cytochrome P-450

Yoshio Goto, Senji Wada, Isao Morishima and Yoshihito Watanabe

J. Inorg. Biochem. **1998**, *69*, 241-247.

2. Mechanism of *N*-Demethylation Catalyzed by High Valent Species of Heme Enzymes: Novel Use of Isotope Effects and Direct Observation of Intermediates

Yoshio Goto, Yoshihito Watanabe, Shunichi Fukuzumi, Jeffrey P. Jones and Joseph P. Dinnocenzo

J. Am. Chem. Soc. **1998**, *120*, 10762-10763.

OTHER PUBLICATIONS

1. Oxidation of Aldehydes by Ferric Peroxo Porphyrin Complexes

Yoshio Goto, Senji Wada, Isao Morishima and Yoshihito Watanabe

J. Inorg. Biochem. **1997**, *67*, 96.

2. Asymmetric Oxidation Catalyzed by Myoglobin Mutants

Shin-ichi Ozaki, Hui-Jung Yang, Toshitaka Matsui, Yoshio Goto, and Yoshihito Watanabe

Tetrahedron Asymm **1998**, in press

3. Mechanisms of Sulfoxidation Catalyzed by High-Valent Intermediates of Heme Enzymes: Electron Transfer vs Oxygen Transfer Mechanism

Yoshio Goto, Shin-ichi Ozaki, Toshitaka Matsui, Yoshihito Watanabe and Shunichi Fukuzumi

J. Am. Chem. Soc. in submission

4. Structure-Function Relationship of Sperm Whale Myoglobin His64Ser Mutant

Yoshio Goto, Shin-ichi Ozaki, Toshitaka Matsui, Yoshihito Watanabe and Shunichi Fukuzumi

in preparation